Missouri University of Science and Technology
Scholars' Mine

Mathematics and Statistics Faculty Research & Creative Works

Mathematics and Statistics

01 Oct 2019

Three-Dimensional Rotation of Paramagnetic and Ferromagnetic Prolate Spheroids in Simple Shear and Uniform Magnetic Field

Christopher A. Sobecki

Yanzhi Zhang
Missouri University of Science and Technology, zhangyanz@mst.edu

Cheng Wang
Missouri University of Science and Technology, wancheng@mst.edu

Follow this and additional works at: https://scholarsmine.mst.edu/math_stat_facwork

 Part of the Mathematics Commons, Mechanical Engineering Commons, and the Statistics and Probability Commons

Recommended Citation

C. A. Sobecki et al., "Three-Dimensional Rotation of Paramagnetic and Ferromagnetic Prolate Spheroids in Simple Shear and Uniform Magnetic Field," *Physics of Fluids*, vol. 31, no. 10, American Institute of Physics (AIP), Oct 2019.
The definitive version is available at https://doi.org/10.1063/1.5123596

This Article - Journal is brought to you for free and open access by Scholars' Mine. It has been accepted for inclusion in Mathematics and Statistics Faculty Research & Creative Works by an authorized administrator of Scholars' Mine. This work is protected by U. S. Copyright Law. Unauthorized use including reproduction for redistribution requires the permission of the copyright holder. For more information, please contact scholarsmine@mst.edu.

Physics of Fluids ARTICLE scitation.org/journal/phf

Three-dimensional rotation of paramagnetic and ferromagnetic prolate spheroids in simple shear and uniform magnetic field

Cite as: Phys. Fluids 31, 102005 (2019); doi: 10.1063/1.5123596
Submitted: 7 August 2019 • Accepted: 25 September 2019 •
Published Online: 14 October 2019

View Online Export Citation CrossMark

Christopher A. Sobecki,[1] Yanzhi Zhang (张燕只),[2] and Cheng Wang (王成)[1,a)]

AFFILIATIONS

[1] Department of Mechanical and Aerospace Engineering, Missouri University of Science and Technology, 400 W. 13th St., Rolla, Missouri 65409, USA
[2] Department of Mathematics and Statistics, Missouri University of Science and Technology, 400 W. 12th St., Rolla, Missouri 65409, USA

[a)] wancheng@mst.edu

ABSTRACT

We examine a time-dependent, three-dimensional rotation of magnetic ellipsoidal particles in a two-dimensional, simple shear flow and a uniform magnetic field. We consider that the particles have paramagnetic and ferromagnetic properties, and we compare their rotational dynamics due to the strengths and directions of the applied uniform magnetic field. We determine the critical magnetic field strength that can pin the particles' rotations. Above the critical field strength, the particles' stable steady angles were determined. In a weak magnetic regime (below the critical field strength), a paramagnetic particle's polar angle will oscillate toward the magnetic field plane while its azimuthal angle will execute periodic rotations. A ferromagnetic particle's rotation depends on its initial angles and the magnetic field strength and direction. Even when it is exposed to a critical magnetic field strength, its rotational dynamics will either be pinned in or out of the magnetic field plane. In a weak magnetic regime, a ferromagnetic particle will either execute out-of-plane rotations or will oscillate toward the magnetic field plane and perform periodic rotations. For both particles, we analytically determine the peaks and troughs of their oscillations and study their time-dependent rotations through analytical and numerical analyses.

Published under license by AIP Publishing. https://doi.org/10.1063/1.5123596

I. INTRODUCTION

Magnetic fields have been gaining popularity as a method of transporting microparticles for a variety of applications similar to electrical fields.[1–3] For example, magnetic forces assist as magnetic separators for mining and biological cells and removing harmful metals to treat water for public health.[4–6] For the biomedical field, magnetic particles have been used in magnetic fields for active drug targeting to convey the magnetic drug to specific parts of the body, improving drug delivery for various diseases such as cancer.[7,8] Some methods of drug targeting include a ferromagnetic stent that attracts ferromagnetic spheres,[7] ferromagnetic nanoparticles in ferrofluids,[8] and separation of cells that include magnetically tagging cells with ferromagnetic or paramagnetic nanobeads.[6] In these situations, magnetic manipulations require magnetic forces to be generated by a spatially nonuniform magnetic field or a magnetic field gradient.[9,10]

Past experimental[11] (studied in two-dimensions), theoretical[12] (studied in two-dimensions), and numerical applications[13,14] (studied in two- and three-dimensions) have validated a novel improvement for manipulating the transportation of nonspherical particles placed in microfluidic devices with low-Reynolds-number flow fields and an applied uniform magnetic field. Most of these articles have studied or applied particles in microchannels that consist of a Pouiselle flow where the Reynolds number is low ($R_e \ll 1$), thus the rotational dynamics of a particle is considered to be very important when studying its lateral migration. In theory, when the particle is at an infinite distance away from the wall, the particle does not experience any net migration and it is free to rotate since inertia is zero. When an ellipsoidal particle is near a wall, there exists a

Published under license by AIP Publishing

particle-wall hydrodynamic interaction, i.e., a lift force, as an effect by the coupling of the rotational and translational motion of the particle. As a result, an ellipsoidal particle will have a nonzero lift velocity that is perpendicular to the wall.[15,16] How much the particle will oscillate depends on the particle-wall distances, the shear rate, and the shape of the particle. Since we can assume there are no external force(s), particle inertia, and the rotation is symmetric, the oscillation motion of the particle after one periodic rotation allows the particle to experience a zero net migration.[11]

Even though a uniform magnetic field does not produce any magnetic forces, a nonspherical particle will experience a magnetic torque in which its rotational dynamics are affected.[17] Ran *et al.* showed the effect of separating ellipsoidal and spherical paramagnetic particles in a low-Reynolds-number flow by applying a uniform magnetic field.[11] Applying a weak magnetic field broke the symmetry of the ellipsoidal particle's periodic rotation in contrast to its rotation in a simple shear flow. The particle-wall interaction allowed the ellipsoidal particle to perform a net migration toward or away from the wall, depending on the magnetic field direction, while the spherical particle's lateral position did not change. Matsunaga *et al.* used a far field theory to evaluate how a permanent (ferromagnetic) magnetic ellipsoid can have its rotation pinned in a stable, steady direction.[13] Depending on how a particle is pinned, for example, near a wall or in a closed channel, the ferromagnetic particle can drift toward or away from the wall. Sobecki *et al.* and Zhang *et al.* showed that by using theoretical and numerical applications, paramagnetic and ferromagnetic ellipsoids can be effectively separated in strong and weak magnetic fields applied in an arbitrary direction.[12,14] Results showed that the rotations of ferromagnetic and paramagnetic particles are pinned at different stable steady angles and their pinned directions resulted in different lateral migration speeds toward or away from the wall. When exposed in a weak magnetic regime, both particles will tend to have different times for one-half of a rotation. Particles tend to oscillate toward and away from the wall in weak magnetic fields or drift away from the wall in strong magnetic fields given their shape.

Although these studies are important for many applications, they may not be applicable to real-world situations that need to be solved in three dimensions. As microfluidic technologies become more advanced and complex, so do the fundamental problems and the solutions that are desired. Gaining interest are organs-on-a-chip and three-dimensional cellular cultures, microfluidic devices that guide drugs in quasihuman environments and can theoretically replace animal testing.[18] Therefore, time-dependent rotation of paramagnetic and ferromagnetic particles in three-dimensional environments and uniform magnetic fields is an important attribute and has been studied significantly in similar studies.[19–24] Effective use of torques to manipulate the rotation of particles is important when considering particle rotational dynamics in simple shear flows, such as when using uniform electric field on ellipsoidal particles[19,24] and a uniform magnetic fields on permanent magnetic particles in simple shear flows or closed channels.[20,21] Even though there have been studies for a particle with a three-dimensional rotation, there currently does not exist a study that compares a time-dependent, three-dimensional rotation between ferromagnetic and paramagnetic particles in simple shear flows and when a strong or weak magnetic field is applied. Our contribution about a three-dimensional rotation can assist future analyses when applying strong and weak magnetic fields on a particle in a rectangular channel.

The knowledge about torques and rotational dynamics of ellipsoidal particles in simple shear flows was developed by Jeffery.[25] Paramagnetic and ferromagnetic particles in uniform magnetic fields, however, requires a fundamental analysis of their respective magnetic torques. Past authors have analyzed dielectric particles in simple shear flows and uniform magnetic fields,[24] along with paramagnetic and ferromagnetic particles.[20,22] Given the contrasting magnetic properties between paramagnetic and ferromagnetic particles, a uniform magnetic field can have different effects on their magnetic torques and ultimately their angular velocities.

In the first part of this research, we will theoretically analyze hydrodynamic torques (with subscripts h) and angular velocities of particles in a shear flow by assuming that the Reynolds number is zero. The initial rotations of an ellipsoid will affect its trajectory including the peak, trough, and amplitudes of the rotations. The particle's azimuthal angle ϕ_h is only affected by the particle's aspect ratio, but the particle's polar angle θ_h is affected by the initial angles $\phi_{h,0}$ and $\theta_{h,0}$, the time dependent rotations of ϕ_h and θ_h, and the particle aspect ratio. In the second and third parts, we study the time-dependent rotations for paramagnetic and ferromagnetic particles in strong and weak magnetic fields, respectively, since their angular velocities have different dependencies. Thus, the paramagnetic (with subscript p) and ferromagnetic (with subscript f) particles' rotations in weak and strong field regimes will behave differently as well. Similar to previous studies, we introduce two dimensionless parameters S_p and S_f to indicate the ratio between the magnetic field strength and the hydrodynamic viscosity and shear rate for paramagnetic and ferromagnetic particles, respectively.[12,14] Given the field strengths S_p and S_f and the magnetic field direction β, the rotational dynamics of paramagnetic and ferromagnetic particles can be manipulated. In strong field regimes (above critical field strengths), particles will be pinned at a stable steady direction in the same plane as the magnetic field, but paramagnetic and ferromagnetic particles will be pinned at different stable steady directions, ϕ_p^s, $\theta_p^s = \pi/2$, and ϕ_f^s, $\theta_f^s = \pi/2$, respectively. In weak magnetic regimes (below the critical field strength), particles can either oscillate toward the same plane as the magnetic field or perform periodic rotations. Given strong or weak magnetic field strength regimes, the magnetic properties of a particle and the initial rotations, we can evaluate the rotation of the particle and determine its peaks, troughs, and amplitudes of its rotation.

II. BACKGROUND OF THE PROBLEM

We consider a simple case for a neutrally buoyant prolate spheroidal particle, shown in Fig. 1. Since the ellipsoid is a micrometer-sized particle, any Brownian effects are assumed negligible. The particle has a semimajor axis a and two semiminor axes b, initial angles ϕ_0 and θ_0, and a constant density ρ_p. The particle is immersed in a nonmagnetic and Newtonian fluid with a constant density ρ_f and dynamic viscosity η with a simple shear flow in the x-z plane. We see that the shear flow, the fluid velocity field gradient, and the vorticity are parallel to the x-, z-, and y-axis, respectively. The velocity of the fluid is $u = \dot{\gamma}z$ with $\dot{\gamma}$ being the shear rate of the

Published under license by AIP Publishing

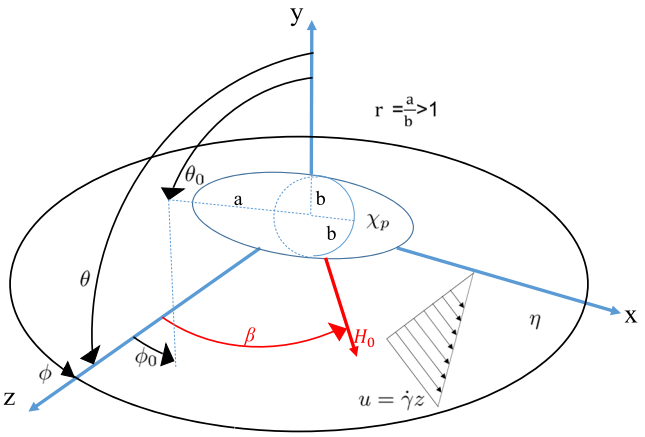

FIG. 1. Schematic of a magnetic prolate ellipsoidal particle with initial angles ϕ_0 and θ_0 in a simple shear flow. A uniform magnetic field is applied in an arbitrary direction β and has a magnetic field strength H_0. The angles denoted as ϕ_h and θ_h will later be used as ϕ_p and θ_p for paramagnetic particles and ϕ_f and θ_f for ferromagnetic particles.

fluid. We further assume that the limit of the Reynolds number of the fluid is zero and thus any fluid or particle inertia are negligible. Also, applied in the x-z plane (i.e., perpendicular to the vorticity) is an external uniform magnetic field $\mathbf{H}_0 = H_0[\sin(\beta), 0, \cos(\beta)]$, where H_0 is its magnitude and β represents the direction of the applied magnetic field measured from the positive z-axis (i.e., perpendicular to the vorticity and parallel to the velocity field gradient). We will describe this region as the magnetic field plane. For a magnetic field direction perpendicular to the vorticity and parallel to the shear flow, $\beta = \pi/2$.

III. HYDRODYNAMIC TORQUE

In the absence of a magnetic field and when the particle's angles are out of the x-z plane, the particle will experience three hydrodynamic torques in a three-dimensional rotation. The torques are due to the simple shear flow in the x-z plane, and the hydrodynamic flow will cause the particle to perform periodic rotations with two angular velocities that are important for this analysis: $\omega_h \mathbf{e}_x = \dot{\theta}_h$ and $\omega_h \mathbf{e}_z = -\sin(\theta_h)\dot{\phi}_h$, where $\dot{\theta}_h$ and $\dot{\phi}_h$ are the hydrodynamic angular velocities for the θ_h and ϕ_h angles, respectively.[19] The hydrodynamic torques in the x and z directions are expressed by an adapted form $\mathbf{L}_h = \mathbf{L}_{h,x} + \mathbf{L}_{h,z}$,[12,19]

$$\mathbf{L}_{h,x} = \frac{2V\eta(r^2+1)}{r^2 D_{xx} + D_{zz}}\left[\dot{\gamma}\frac{(r^2-1)\sin(2\phi_h)\sin(2\theta_h)}{4(r^2+1)} - \dot{\theta}_h\right]\mathbf{e}_x, \quad (1)$$

$$\mathbf{L}_{h,z} = \frac{-2V\eta(r^2+1)\sin(\theta_h)}{r^2 D_{xx} + D_{zz}}\left[\dot{\gamma}\frac{r^2\cos^2(\phi_h) + \sin^2(\phi_h)}{r^2+1} - \dot{\phi}_h\right]\mathbf{e}_z, \quad (2)$$

where $V = \frac{4}{3}\pi ab^2$ is the volume of the particle, $r = a/b$ is the aspect ratio, and D_{xx} and D_{zz} are considered to be the diagonal components of the demagnetization factors. In the equations above, we identify our demagnetization factors as $D_{xx} = 1 - A$ and $D_{zz} = \frac{A}{2}\left(\text{where } A = \frac{r^2}{(r^2-1)} - \frac{r\cosh^{-1}(r)}{(r^2-1)^{3/2}}\right)$. We will apply them later when we find the total torque that considers the sum of the hydrodynamic and magnetic torques acting on the ellipsoidal particle.[26] By setting the hydrodynamic torques to zero, the hydrodynamic angular velocities can be rewritten in the dimensionless form of the well-known Jeffery orbits,[12,25,27]

$$\dot{\phi}_h = \frac{r^2\cos^2(\phi_h) + \sin^2(\phi_h)}{r^2+1}, \quad (3)$$

and

$$\dot{\theta}_h = \frac{(r^2-1)\sin(2\phi_h)\sin(2\theta_h)}{4(r^2+1)}, \quad (4)$$

where $\dot{\phi}_h = \frac{d\phi_h}{dt^*}$, $\dot{\theta}_h = \frac{d\theta_h}{dt^*}$, and $t^* = t\dot{\gamma}$ is the period of rotation. Integrating Eq. (3) yields[25,27,28]

$$\tan(\phi_h) = r\tan\left(\frac{2\pi t^*}{T_h} + \left(\arctan\left[\frac{\tan(\phi_{h,0})}{r}\right] + k_1\pi\right)\right), \quad (5)$$

where $k_1 = 0$ or 1, which makes the arc-tangent parameter lie between 0 and π, $T_h = \frac{2\pi(r^2+1)}{r}$ is the dimensionless period for one full rotation, and $\phi_{h,0}$ is the initial azimuthal angle ϕ_h. Since the polar angle θ_h is dependent on the azimuthal angle ϕ_h, dividing Eqs. (4) and (3)and integrating yields[25,28]

$$\tan(\theta_h) = \tan(\theta_{h,0})\sqrt{\frac{r^2\cos^2(\phi_{h,0}) + \sin^2(\phi_{h,0})}{r^2\cos^2(\phi_h) + \sin^2(\phi_h)}}, \quad (6)$$

where $\theta_{h,0}$ is the initial polar angle θ_h. If $\theta_{h,0} \neq 0$ or $\pi/2$, then θ_h will oscillate between its peaks and troughs found on the θ_h-curve when we set Eq. (5) at $\theta_{h,max}$ (at $\phi_h = \pi/2$ or $3\pi/2$) and $\theta_{h,min}$ (at $\phi_h = 0$ or π and 2π) respectively.[29] We can thus find the amplitude for θ_h ($\theta_{h,amp} = \theta_{h,max} - \theta_{h,min}$). For the hydrodynamic case, $\theta_{h,amp}$ remains positive except for special cases when $\theta_{h,0} = 0$ (a rolling log) and $\theta_{h,0} = \frac{\pi}{2}$ (a particle rotating in the shear flow).

IV. MAGNETIC TORQUES

In the presence of a uniform magnetic field strength $\mathbf{H}_0$, the particle will experience a magnetic torque $\mathbf{L}_m = \mu_0(\mathbf{m} \times \mathbf{H}_0)$, where $\mathbf{m}$ is the magnetic moment of the particle and μ_0 is the magnetic permeability of free space. A uniform magnetic field affects paramagnetic and ferromagnetic particles differently. The magnetic moment of a paramagnetic particle is an internal field that is induced by the external magnetic field, whereas the magnetic moment of a ferromagnetic particle has a constant magnetization $\mathbf{M}_0$. The magnetic torques will be different even if they are both ellipsoids with the same aspect ratios.

V. PARAMAGNETIC PARTICLE

We assume a paramagnetic particle is homogeneous and linearly magnetizable when exposed to a uniform magnetic field, and thus $\mathbf{m} = \chi V\mathbf{H}^-$, where χ is the magnetic susceptibility and $\mathbf{H}^-$ is the internal magnetic field of the particle. The particle can have its rotational dynamics affected by a magnetic field, and we can find the total magnetic torque, $\mathbf{L}_{mp} = \mathbf{L}_{mp,x} + \mathbf{L}_{mp,z}$, since $\mathbf{L}_{mp,y} = 0\mathbf{e}_y$,[12,17,19]

Published under license by AIP Publishing

$$\mathbf{L}_{mp,x} = \frac{V\chi^2\mu_0 H_0^2 (D_{xx} - D_{zz}) \cos^2(\phi_p - \beta) \sin(2\theta_p)}{2(1+\chi D_{xx})(1+\chi D_{zz})} \mathbf{e}_x, \quad (7)$$

$$\mathbf{L}_{mp,z} = -\frac{V\chi^2\mu_0 H_0^2 (D_{xx} - D_{zz}) \sin(2\phi_p - 2\beta) \sin(\theta_p)}{2(1+\chi D_{xx})(1+\chi D_{zz})} \mathbf{e}_z, \quad (8)$$

where ϕ_p and θ_p describe the angles of a paramagnetic particle. Since the torque with respect to the vorticity is zero, we can ignore it for our analysis. By adding the magnetic and hydrodynamic torques and equating them to zero ($\mathbf{L}_h + \mathbf{L}_{mp} = 0$), we can find our two angular velocities[19]

$$\dot{\phi}_p = \frac{r^2 \cos^2(\phi_p) + \sin^2(\phi_p) - S_p \sin(2\phi_p - 2\beta)}{r^2 + 1}, \quad (9)$$

and

$$\dot{\theta}_p = \frac{(r^2 - 1) \sin(2\phi_p) \sin(2\theta_p) + 4S_p \cos^2(\phi_p - \beta) \sin(2\theta_p)}{4(r^2 + 1)}, \quad (10)$$

where $S_p = \frac{\mu_0\chi^2 H_0^2 \lambda}{\eta\dot{\gamma}}$, with $\lambda = \frac{(D_{zz}-D_{xx})(r^2 D_{xx}+D_{zz})}{4(1+\chi D_{xx})(1+\chi D_{zz})}$, is a dimensionless variable that describes a ratio between the magnetic and hydrodynamic strengths and is the same variable definition as in previous works.[11,12] We can observe that the equations above are periodic in ϕ_p with period π because of the symmetrical rotation of the paramagnetic prolate spheroid given by $\sin(2\phi_p - 2\beta)$ in Eq. (9) and $\cos^2(\phi_p - \beta)$ in Eq. (10). For θ_p, the boundary is set at $(0, \pi/2]$. Hence, any magnetic field magnetic direction $\beta + \pi$ will have the same torque and particle motion as β for the same ϕ_p and θ_p angles.

The value of the dimensionless variable S_p, however, describes the magnetic effects on the orientation of the particle. If S_p is very large, then the particle will be pinned at a stable steady angle and is almost parallel to the magnetic field direction. As the magnetic field strength decreases, the particle's angular velocity will be affected by the magnetic field strength and direction and the particle's angular position. To further analyze our dimensionless variable, at an arbitrary magnetic field direction, we can find the critical field strength (S_p^{cr}) that can pin the particle at two critical angles ϕ_p^{cr} and θ_p^{cr}. We can then observe the dimensionless time dependency of the particle oscillating from its out-of-plane position to the magnetic field that lies on the xz-plane.

A. Paramagnetic particle in strong magnetic field

A paramagnetic particle in a strong field regime must meet the condition that $Q = \sqrt{S_p^2 + S_p(r^2 - 1)\sin(2\beta) - r^2}$ is real. The analytic solution for $\tan(\phi_p)$ can be founded by integrating Eq. (9) to find our time-dependent rotation[19]

$$\tan(\phi_p) = \frac{S_p \cos(2\beta) + Q \tanh\left(-\frac{Qt^*}{r^2+1} + \tanh^{-1}\left[\frac{\tan(\phi_{p,0})(1 - S_p \sin(2\beta)) - S_p \cos(2\beta)}{Q} \right] \right)}{1 - S_p \sin(2\beta)}. \quad (11)$$

By dividing Eqs. (9) and (10) and integrating,[19]

$$\tan(\theta_p) = \tan(\theta_{p,0}) \sqrt{\frac{r^2 \cos^2(\phi_{p,0}) + \sin^2(\phi_{p,0}) - S_p \sin(2\phi_{p,0} - 2\beta)}{r^2 \cos^2(\phi_p) + \sin^2(\phi_p) - S_p \sin(2\phi_p - 2\beta)}} \exp\left(\frac{S_p t^*}{r^2 + 1} \right). \quad (12)$$

Equations (11) and (12) show that when $S_p \to \infty$, the particle's semi-major axis will be pinned at a stable equilibrium solution parallel to the magnetic field direction.

For a particle in a strong magnetic regime, the total angular velocity will be zero, and the particle will be pinned at in a neutrally stable direction when $S_p = S_p^{cr}$ ($Q = 0$) and a stable steady angle when $S_p^{cr} < S_p$ ($0 < Q$).[12] However, the particle will be pinned at a stable steady direction on the magnetic field plane when $t^* \to \infty$ in Eq. (11),[11,12]

$$\tan(\phi_p^s) = \frac{S_p \cos(2\beta) - Q}{1 - S_p \sin(2\beta)}, \quad (13)$$

which is the same equation from Zhou *et al.* and Sobecki *et al.*[11,12] By setting $Q = 0$, the critical strength S_p^{cr} yields

$$S_p^{cr} = \frac{1}{2}\left[\sqrt{(r^2 - 1)^2 \sin^2(2\beta) + 4r^2} - (r^2 - 1)\sin(2\beta) \right]. \quad (14)$$

Thus, Eq. (13) can be re-expressed at the critical field strength

$$\tan(\phi_p^{cr}) = \frac{S_p^{cr} \cos(2\beta)}{1 - S_p^{cr} \sin(2\beta)}. \quad (15)$$

The critical/stable steady angles and the critical field strengths can be further observed from other studies.[11,12,14]

When $S_p = S_p^{cr}$, there does not exist a periodic rotation as analyzed in Eq. (11).

Figure 2 shows the time-dependent rotation for $r = 4$ and magnetic field strengths above the critical, $S_p = S_p^{cr} + 1$, for each of the magnetic field directions and at initial angles $\phi_{p,0} = 0$ and $\theta_{p,0} = \pi/10$. We then combine the particle's rotations on a rotation sphere to observe the effect of a particle in a three-dimensional trajectory in Fig. 2(c). A paramagnetic particle exposed to a magnetic field $\beta = 3\pi/4$ with the strength of $S_p = 17$ will have its polar angle θ_p rotate toward $\pi/2$ quicker than all other magnetic field directions

Published under license by AIP Publishing

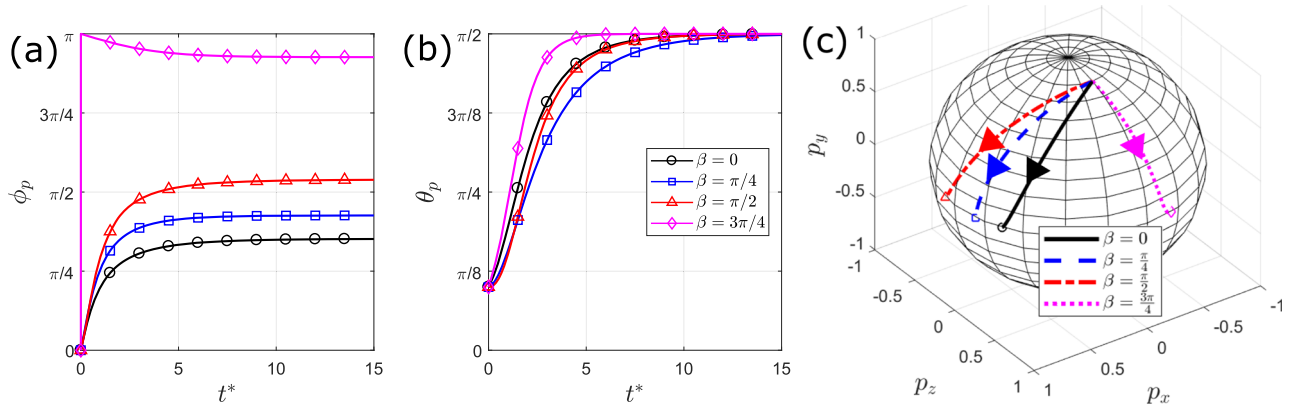

FIG. 2. Time-dependent rotation of a paramagnetic particle under various magnetic field directions and their respective magnetic strengths $S_p = S_p^{cr} + 1$ for (a) the particle's azimuthal angle ϕ_p with respect to time, (b) the particle's polar angle θ_p with respect to time, and (c) the rotation sphere that studies the particle's trajectory as a result from (a) and (b). The initial angles are $\phi_{p,0} = 0$ and $\theta_{p,0} = \pi/10$.

and strengths even when they begin from the same initial angles. This is given from the polar angle θ_p becoming dependent on the particle's azimuthal angle ϕ_p. The particle exposed to a magnetic field direction $\beta = 3\pi/4$ will rotate backward toward its steady stable direction, while all other magnetic field directions shown will rotate forward to their respective stable steady states. Given the azimuthal angle ϕ_p and the dimensionless time that it takes to approach between $\phi_{p,0} < \phi_p < \phi_p^s$, the particle's polar angle θ_p will approach the magnetic field plane faster. We can make an observation from Eqs. (11)–(13) and from Fig. 2 that for all aspect ratios and magnetic field strengths and directions, how quickly a particle rotates toward its steady stable state will depend on the initial position of the particle.

B. Paramagnetic particle in weak magnetic field

In a weak field regime, $0 < S_p < S_p^{cr}$, a paramagnetic spheroid's azimuthal angle ϕ_p will complete asymmetric periodic rotations, but the rotational period increases as S_p approaches S_p^{cr}. Its polar angle θ_p, however, will oscillate toward $\pi/2$, and the particle will rotate in the x-z plane (i.e., a two-dimensional rotation) as $t^* \to \infty$. A particle is in a weak field regime if $g = |Q|$, where Q is an imaginary number. We obtain the equation by integrating Eq. (9),

$$\tan(\phi_p) = \frac{S_p \cos(2\beta) + g \tan\left(\frac{2\pi t^*}{T_p} + \arctan\left[\frac{\tan(\phi_{p,0})(1 - S_p \sin(2\beta)) - S_p \cos(2\beta)}{g}\right] + k_1\pi\right)}{1 - S_p \sin(2\beta)}, \tag{16}$$

where $T_p = \frac{2\pi(r^2+1)}{g}$ is the periodic time for a particle in a weak magnetic field. The rotation for $\tan(\theta_p)$ in a weak magnetic field is the same as Eq. (12).

This theory can be closely observed in Fig. 3 when we study a paramagnetic particle rotating for both angles ϕ_p in (a) and θ_p in (b) when $r = 4$, $S_p = 0.5$, $\phi_{p,0} = 0$, $\theta_{p,0} = \pi/10$, and the magnetic field directions are $\beta = 0$, $\beta = \pi/4$, $\beta = \pi/2$, and $\beta = 3\pi/4$ for (a)–(c), (d)–(f), (g)–(i), and (j)–(l), respectively. We can observe that since the magnetic field strength is closer to the critical field strength for $\beta = \pi/4$ ($S_p^{cr} = 1$), T_p has increased, and consequently the particle's polar angle θ_p requires fewer oscillations to approach a quasisteady state on the same plane as the magnetic field. Further observation can be made on the rotation sphere in Fig. 3(c). This is then compared to a magnetic field direction $\beta = 3\pi/4$ whose critical field strength is larger ($S_p^{cr} = 16$) and requires more oscillations to have a particle's polar angle θ_p approach faster toward the magnetic field plane.

Their time-dependent rotation is based on the polar angle's oscillations by trying to find its peaks and troughs. In order to know the amplitude on the particle's polar angle θ_p for each completed periodic rotation, we would need to know exactly what ϕ_p value would cause $\dot{\theta}_p = 0$ assuming that $\theta_p \neq 0$ or $\pi/2$ and $\dot{\phi}_p \neq 0$. By setting Eq. (10) to zero, we obtain

$$\tan(\phi_p^{\pm}) = \frac{1 - r^2 - 2S_p \sin(2\beta) \pm \sqrt{(r^2-1)(r^2 - 1 + 4S_p \sin(2\beta))}}{4 \sin(\beta)^2 S_p} \tag{17}$$

Published under license by AIP Publishing

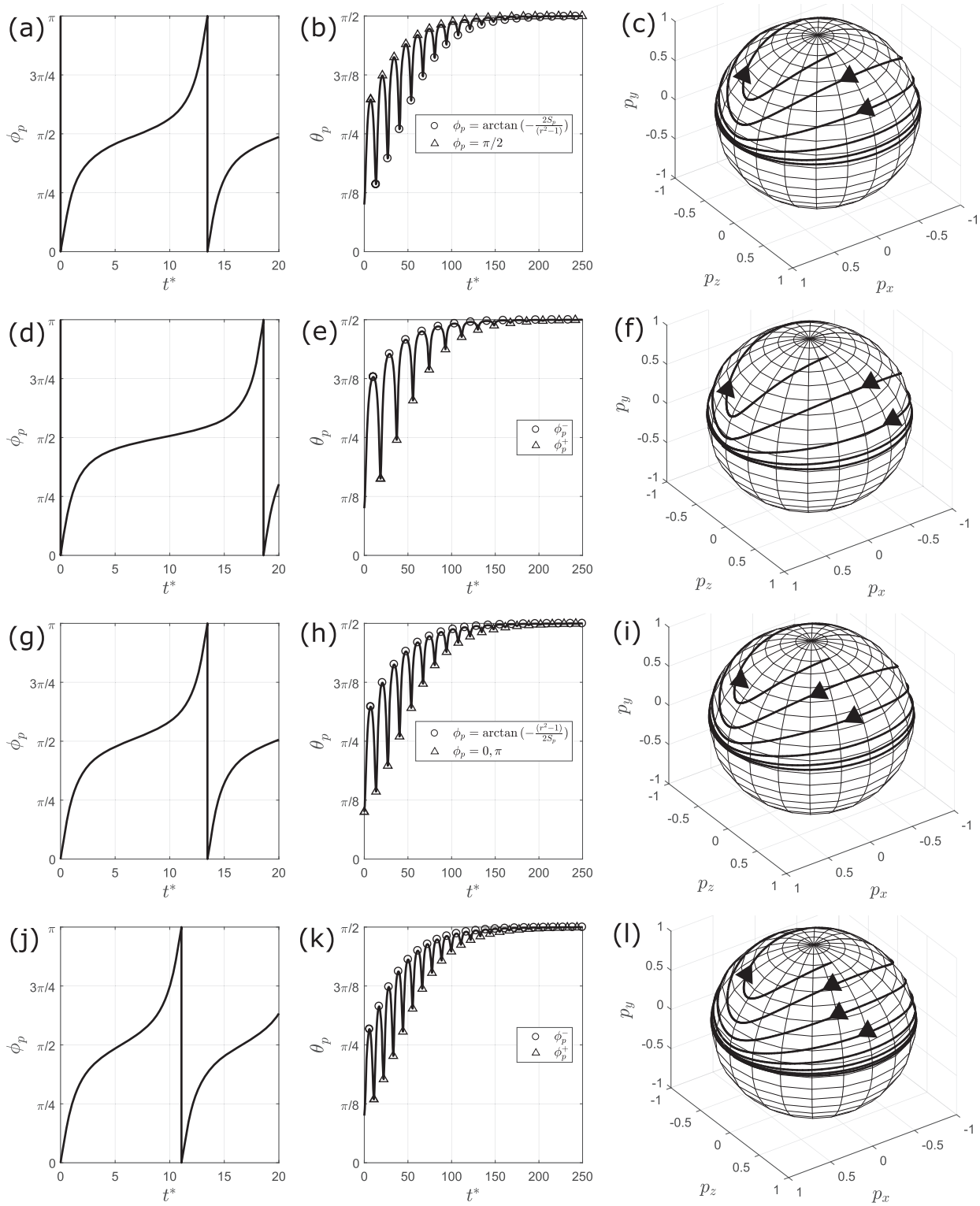

FIG. 3. Time-dependent rotation of paramagnetic particles in a weak field regime (S_p = 0.5) for ϕ_p and θ_p, and their trajectories for [(a)–(c)] β = 0, [(d)–(f)] $\beta = \pi/4$, [(g)–(i)] $\beta = \pi/2$, and [(j)–(l)] $\beta = 3\pi/4$. Each of the symbols in (b), (e), (h), and (k) represents the azimuthal angle ϕ_p that results $\dot{\theta}_p = 0$, but $\dot{\phi}_p \neq 0$.

Published under license by AIP Publishing

for arbitrary magnetic field directions. For some magnetic field directions, even if the field strength is $S_p < S_p^{cr}$, the square-root parameter can still become nonreal, indicating that $\dot{\theta} \neq 0$ as $\theta_p \to \pi/2$ (i.e., there are no oscillations as the particle approaches the magnetic field plane). For $\beta = 0$, π, and $\pi/2$, we have

$$\tan(\phi_{p,\beta=0,\pi}) = \frac{-2S_p}{r^2-1} \text{ or } \phi_p = \pi/2, \tag{18}$$

$$\tan(\phi_{p,\beta=\pi/2}) = -\frac{r^2-1}{2S_p} \text{ or } \phi_p = 0, \pi. \tag{19}$$

Thus, from Eq. (16), we can find the oscillation time δ to satisfy $\dot{\theta}_p = 0$,

$$\delta = \frac{r^2+1}{g}\left\{\left[\arctan\left(\frac{\tan(\phi_p)(1-S_p\sin(2\beta)) - S_p\cos(2\beta)}{g}\right) + k_1\pi\right] - \left[\arctan\left(\frac{\tan(\phi_{p,0})(1-S_p\sin(2\beta)) - S_p\cos(2\beta)}{g}\right) + k_2\pi\right]\right\}, \tag{20}$$

where $k_1 = 0$ or 1 and $k_2 = 0$ or 1 to keep the first and second arc-tangent functions between 0 and π. We can replace $\tan(\phi_p)$ in Eq. (16) with $\tan(\phi_p^{\pm})$, $\tan(\phi_{p,\beta=0,\pi})$, or $\tan(\phi_{p,\beta=\pi/2})$ and set $t^* = \delta$ at these oscillations. To find the period of rotations for the additional peaks and troughs, we would add nT_p to Eq. (20) where n is a non-negative integer and $n = (0, 1)$ corresponds to the first peak or trough. If we want to find the particle's polar angles θ_p at these specific times, we would plug in the results from Eqs. (17) and (18), or (19), along with (20) into Eq. (12). As $t^* \to \infty$, $\theta_p = \pi/2$, but we can establish a quasisteady state for an amplitude that is less than one, and the peaks of the two consecutive amplitudes are divided by $\pi/2$ and have an error less than 1. Figure 3(f) shows the rotation sphere for $\beta = \pi/4$ when we combine our ϕ_p- and θ_p-rotations. Since the weak magnetic field strength is closer to the critical field strength of the respected magnetic field, and since the number of oscillations approaching $\pi/2$ is minimal, the number of rotations around the rotation sphere has decreased as well compared to all of the other magnetic field directions.

VI. FERROMAGNETIC PARTICLE

Similar to a paramagnetic particle, we can calculate the magnetic torque on a ferromagnetic particle when assuming that its magnetization $\mathbf{M}_0$ is parallel to its major axis. The magnetic moment applied on a ferromagnetic particle is $\mathbf{m} = V\mathbf{M}_0 = V\,M_0[\sin(\phi_f)\sin(\theta_f), \cos(\theta_f), \cos(\phi_f)\sin(\theta_f)]$ with M_0 denoting the magnitude of its magnetization. The magnetic torque on a ferromagnetic particle is $\mathbf{L}_{mf}$. The magnetic torque in the y direction is zero $\mathbf{L}_{mf,y} = 0\mathbf{e}_y$, but the torques for the x and z directions are

$$\mathbf{L}_{mf,x} = \mu_0 V M_0 H_0 \cos(\theta_f)\cos(\phi_f - \beta)\mathbf{e}_x, \tag{21}$$

$$\mathbf{L}_{mf,z} = \mu_0 V M_0 H_0 \sin(\phi_f - \beta)\mathbf{e}_z, \tag{22}$$

where θ_f and ϕ_f are the angles of a ferromagnetic particle. Then, by adding the hydrodynamic and ferromagnetic angular torques to zero ($\mathbf{L}_h + \mathbf{L}_{m,f} = 0$), we can find the total angular velocities,[20]

$$\dot{\phi}_f = \frac{[r^2\cos^2(\phi_f) + \sin^2(\phi_f)]\sin(\theta_f) - S_f\sin(\phi_f - \beta)}{(r^2+1)\sin(\theta_f)}, \tag{23}$$

$$\dot{\theta}_f = \frac{(r^2-1)\sin(2\phi_f)\sin(2\theta_f) + 4S_f\cos(\theta_f)\cos(\phi_f - \beta)}{4(r^2+1)}, \tag{24}$$

where $S_f = \frac{\mu_0 M_0 H_0 (r^2 D_{xx} + D_{zz})}{2\eta\dot{\gamma}}$ and describes the ratio between magnetic and hydrodynamic effects. As opposed to a paramagnetic particle's dimensionless variable S_p, S_f is nonzero for spherical particles ($r = 1$).

A. Stability analysis of steady angles

Since Eqs. (23) and (24) is a nonlinear system, it would be challenging to find its analytical solution. Therefore, we use the Runge-Kutta 4 method (RK4) to calculate the time evolution of θ_f and ϕ_f numerically. To analyze the nonlinear dynamics of the ferromagnetic particle, we must analyze our numerical results and the angular velocities from Eqs. (23) and (24) using the Lyaponov theorem in spherical coordinates.[20] The eigenvalues that will depend on the stability of the critical and stable steady angles can be represented by ζ_1 and ζ_2,

$$\zeta_{1,2} = \frac{-(r^2-1)\tan(\phi_f^{cr})\sin^2(\theta_f^{cr}) \pm \Omega}{2(r^2+1)(1+\tan^2(\phi_f^{cr}))}, \tag{25}$$

where $\Omega = \sqrt{(r^2-1)^2\tan^2(\phi_f^{cr})\sin^4(\theta_f^{cr}) - 4r^2(1-\sin^2(\theta_f^{cr}))(1+\tan^2(\phi_f^{cr}))^2}$. Thus, if the real part of both eigenvalues is positive, then ϕ_f^{cr} and θ_f^{cr} are deemed as unstable. If the eigenvalues are both negative, then our critical angles are stable and the particle may perform periodic rotations around the point ϕ_f^{cr} and θ_f^{cr} depending on the magnetic field direction and strength range. In this case, if $\theta_{f,0} \neq \pi/2$, then the particle will perform a rotation toward ϕ_f^{cr} and θ_f^{cr}. If both eigenvalues are zero, then they are neutrally stable. Before we further discuss the analysis of the strong and weak magnetic field subsections, we divide our studies into three cases: $\dot{\phi}_f = 0$ and $\dot{\theta}_f = 0$, $\dot{\phi}_f = 0$ and $\dot{\theta}_f \neq 0$, and $\dot{\phi}_f \neq 0$ and $\dot{\theta}_f = 0$.

1. $\dot{\phi}_f = 0$ and $\dot{\theta}_f = 0$

To impede the particle rotation ($\dot{\phi}_f = \dot{\theta}_f = 0$) for any magnetic field direction, magnetic field strength, and particle aspect ratio, we can determine a ferromagnetic's critical angles,[20]

$$\tan(\phi_f^{cr}) = -r^2\cot(\beta), \tag{26}$$

$$\sin(\theta_f^{cr}) = \pm S_f\frac{\sqrt{\sin^2(\beta) + r^4\cos^2(\beta)}}{r^2}. \tag{27}$$

If we want to find the maximum critical field strength of Eq. (27), then the maximum limit is

$$S_f^{cr,max} = \frac{r^2}{\sqrt{\sin^2(\beta) + r^4\cos^2(\beta)}}. \tag{28}$$

Published under license by AIP Publishing

Otherwise, Eq. (27) will become indeterminate. For magnetic field strengths less than the maximum value, the critical directions are stable for $\pi/2 < \beta < \pi$ ($3\pi/2 < \beta < 2\pi$) and unstable for $0 < \beta < \pi/2$ ($\pi < \beta < 3\pi/2$).[20] When the critical magnetic field strength is at its maximum, the critical angles will be neutrally stable at $\theta_f^{cr} = \pi/2$ and at ϕ_f^{cr}. The maximum strength needed to pin the particles when $\beta = \pi/2$ and $3\pi/2$ is $S_f^{cr} = r^2$, and the minimum strength needed to pin the particles when $\beta = 0$ and $\beta = \pi$ is $S_f^{cr} = 1$. We can find their respective stability from the eigenvalues gained from Eqs. (26) and (27).

2. $\dot{\phi}_f = 0$ and $\dot{\theta}_f \neq 0$

For the second analysis, there are special cases that the particle direction will have one of the angular velocities become zero. In this case, we find the particles' θ_f peaks, troughs, and amplitudes. The special cases are when the magnetic field is perpendicular to the vorticity and perpendicular ($\beta = 0$ and $\beta = \pi$) or parallel ($\beta = \pi/2$ and $3\pi/2$) to the shear flow. For a general magnetic field direction that is not perpendicular or parallel to the shear flow, we can find the polar angle θ_f that will allow $\dot{\phi}_f = 0$. By setting Eq. (23) to zero, we can find[20]

$$\sin(\theta_f) = \frac{S_f \sin(\phi_f - \beta)}{r^2 \cos^2(\phi_f) + \sin^2(\phi_f)}, \tag{29}$$

which yields a quartic equation for $\tan(\phi_f)$ that needs to be solved

$$a_4(\tan(\phi_f))^4 + a_3(\tan(\phi_f))^3 + a_2(\tan(\phi_f))^2 + a_1\tan(\phi_f) + a_0 = 0, \tag{30}$$

where the coefficients $a_0 = r^4\sin^2(\theta_f) - \sin^2(\beta)S_f^2$, $a_1 = a_3 = S_f^2\sin(\beta)$, $a_2 = 2r^2\sin^2(\theta_f) - S_f^2$, and $a_4 = \sin^2(\theta_f) - S_f^2\cos^2(\beta)$. If $\theta_f = \frac{\pi}{2}$, then we will have the same equation as our previous article for a two-dimensional rotation.[12] If $a_4 \neq 0$, Eq. (30) admits four solutions for $\tan(\phi_f)$,

$$\begin{aligned}[\tan(\phi_f)]_{1a,2a} &= -\frac{a_3}{4a_4} - w \pm \frac{1}{2}\sqrt{-4w^2 - 2p + \frac{q}{w}},\\ [\tan(\phi_f)]_{3a,4a} &= -\frac{a_3}{4a_4} + w \pm \frac{1}{2}\sqrt{-4w^2 - 2p - \frac{q}{w}},\end{aligned} \tag{31}$$

where from the "±" notation, the subnotations $1a$ and $3a$ represents the "+" notation and $2a$ and $4a$ represents the "−" notation respectively, and where

$$\begin{aligned}p &= \frac{8a_4a_2 - 3a_3^2}{8a_4^2},\ q = \frac{a_3^3 - 4a_4a_3a_2 + 8a_4^2a_1}{8a_4^3},\\ w &= \tfrac{1}{2}\sqrt{-\frac{2p}{3} + \frac{1}{3a_4}\left(k + \frac{\delta_0}{k}\right)},\\ k &= \sqrt[3]{\frac{\delta_1 + \sqrt{\delta_1^2 - 4\delta_0^3}}{2}},\ \delta_0 = a_2^2 - 3a_1a_3 + 12a_0a_4,\\ \delta_1 &= 2a_2 - 9a_1a_2a_3 + 27a_3^2a_0 + 27a_4a_4a_1^2 - 72a_0a_2a_4.\end{aligned}$$

We will now consider two special cases: (1) a magnetic field perpendicular ($\beta = 0$, π) and (2) parallel ($\beta = \pi/2$, $3\pi/2$) to the shear flow. Following similar procedures as the previous case, for $\beta = 0$ and $\beta = \pi$, our solutions are

$$\begin{aligned}[\tan(\phi_f)]_{1a,2a} &= \pm\sqrt{\frac{(S_f^2 - 2r^2\sin^2(\theta_f)) + S_f\sqrt{S_f^2 + 4r^2(r^2-1)\sin^2(\theta_f)}}{1 - 2S_f^2 - \cos(2\theta_f)}},\\ [\tan(\phi_f)]_{3a,4a} &= \pm\sqrt{\frac{(S_f^2 - 2r^2\sin^2(\theta_f)) - S_f\sqrt{S_f^2 + 4r^2(r^2-1)\sin^2(\theta_f)}}{1 - 2S_f^2 - \cos(2\theta_f)}}.\end{aligned} \tag{32}$$

For $\beta = \pi/2$ and $3\pi/2$,

$$\begin{aligned}[\tan(\phi_f)]_{1a,2a} &= \pm\sqrt{\frac{(S_f^2\csc^2(\theta_f) - 2r^2) + S_f\csc^2(\theta_f)\sqrt{2 - 2r^2 + S_f^2 + 2(r^2-1)\cos(2\theta_f)}}{2}},\\ [\tan(\phi_f)]_{3a,4a} &= \pm\sqrt{\frac{(S_f^2\csc^2(\theta_f) - 2r^2) - S_f\csc^2(\theta_f)\sqrt{2 - 2r^2 + S_f^2 + 2(r^2-1)\cos(2\theta_f)}}{2}}.\end{aligned} \tag{33}$$

When $\theta_f = \frac{\pi}{2}$ in Eqs. (32) and (33), we receive the same set of equations as our previous paper.[12]

3. $\dot{\phi}_f \neq 0$ and $\dot{\theta}_f = 0$

For the third analysis, we use the same method to find the peaks, troughs, and amplitudes as Subsection V B for a general magnetic field direction, a magnetic field that is perpendicular to the shear flow, and a magnetic field parallel to the shear flow. By setting Eq. (24) to zero, we can find the solution for the polar angle θ_f to make this condition true,[20]

$$\sin(\theta_f) = \frac{-S_f\cos(\phi_f - \beta)}{(r^2 - 1)\sin(\phi_f)\cos(\phi_f)}. \tag{34}$$

Published under license by AIP Publishing

For a general magnetic field direction, we can find the ϕ_f-rotations that allows $\dot{\phi}_f = 0$ depending on the θ_f-rotations,

$$b_4(\tan(\phi_f))^4 + b_3(\tan(\phi_f))^3 + b_2(\tan(\phi_f))^2 + b_1\tan(\phi_f) + b_0 = 0, \tag{35}$$

where the coefficients $b_0 = \cos^2(\beta)$, $b_1 = b_3 = \sin(2\beta)$, $b_2 = 1 - \frac{(r^2-1)^2\sin^2(\theta_f)}{S_f^2}$, and $b_4 = \sin^2(\beta)$. To find the real solutions, we use the quartic-formula from Eq. (31) by replacing our "a" coefficients with our "b" coefficients. For the magnetic field perpendicular to the shear flow, we can reduce our solution

$$[\tan(\phi_f)]_{1b,2b} = \pm\frac{S_f}{\sqrt{\sin^2(\theta_f)(r^2-1)^2 - S_f^2}}, \quad \phi_{f,3b} = \pi/2,\ \phi_{f,4b} = 3\pi/2, \tag{36}$$

and

$$[\tan(\phi_f)]_{1b,2b} = \pm\frac{\sqrt{\sin^2(\theta_f)(r^2-1)^2 - S_f^2}}{S_f}, \quad \phi_{f,3b} = 0 \text{ or } 2\pi,\ \phi_{f,4b} = \pi, \tag{37}$$

for a magnetic field parallel to the shear flow. For both equations, we can find $\phi_{f,1b}$ and $\phi_{f,2b}$ if $0 < S_f \le (r^2 - 1)$. In Secs. VI B and VI C, we will analyze these three cases for a particle with aspect ratios $1 < r \le \sqrt{2}$ and $\sqrt{2} < r$ in strong and weak magnetic field regimes applied perpendicular and parallel to the shear flow. These ranges of aspect ratios describe the number of steady angles for a ferromagnetic particle in a two-dimensional shear rate; a particle with an aspect ratio range $1 < r \le \sqrt{2}$ has two possible steady angles, and $\sqrt{2} < r$ can have either four or two steady angles depending on S_f.[12]

B. Ferromagnetic particles in strong magnetic field

In a strong field regime, a ferromagnetic particle impedes in a direction on the x-z plane or in an out-of-plane critical direction given by Eqs. (36) and (37). In our previous paper, we studied S_f^{cr} and ϕ_f^{cr} for aspect ratios $1 < r \le \sqrt{2}$ and $\sqrt{2} < r$ using analytical methods for the magnetic field perpendicular and parallel to the shear rate, and we used the bisection and RK4 methods for all other directions.[12] For any magnetic field direction, when $\frac{r^2}{\sqrt{\sin^2(\beta)+r^4\cos^2(\beta)}} < S_f$, $\theta_f \to \pi/2$ and $\phi_f \to \phi_f^s$ from the particle's initial angles. Since the particle will project toward the same plane as the magnetic field, we set $\dot{\theta}_f = 0$ and Eq. (23) will result in a two-dimensional equation given by our previous study.[12] In this subsection, we will analyze the rotation of the particle for a magnetic field direction perpendicular and parallel to the shear flow.

1. Parallel to the velocity field gradient $\beta = 0$

For a magnetic field perpendicular to the shear flow, a particle will project toward $\theta_f = \pi/2$ and $\phi_f = \phi_f^s$ in a strong field regime ($S_f^{cr} < S_f$). In this case, we rely on Eq. (32) to find the steady angles after setting $\theta_f = \pi/2$. We see in Fig. 4 that the stable steady angles for (a) $r = 1.4$ and (b) $r = 4$ and magnetic field strength of $S_f = 2$ are $\phi_{f,3a}$ and $\phi_{f,4a}$ at $\theta_f = \pi/2$ because the respective angular velocities are $\dot{\phi}_f = 0$ and $\dot{\theta}_f = 0$ at the same points. Additionally, in Fig. 4, we can determine if the rates of the angular velocities in each region in (a) and (b) are both negative, positive, or a mix simply by evaluating the angular velocities in those regions and by observing the time-dependent rotations. Since we see in Figs. 5(a) and 5(d) that if the particle approaches $\phi_{f,3a}$ and since $\frac{d\dot{\phi}_f}{d\phi_f}\Big|_{\substack{\theta_f=\pi/2\\ \phi_f=\phi_{f,3a}}} < 0$, then $\phi_{f,3a}$ is a stable steady angle, whereas $\phi_{f,4a}$ is unstable since $0 < \frac{d\dot{\phi}_f}{d\phi_f}\Big|_{\substack{\theta_f=\pi/2\\ \phi_f=\phi_{f,4a}}}$. Additionally, there exists two $\phi_{f,b}$-values for aspect ratios $1 < r \le \sqrt{2}$, where $\dot{\phi}_{f,b} \neq 0$ but $\dot{\theta}_f = 0$, $\phi_{f,3b}$ and $\phi_{f,4b}$, because $r^2 - 1 < S_f$ for $S_f^{cr} < S_f$. For $\sqrt{2} < r$, there exists four ϕ_f-values.

In Fig. 5, we observe the time dependency for our angles ϕ_f in (a) and θ_f in (b) for (a)–(c) $r = 1.4$ and (d)–(f) $r = 4$. The initial angles are $(\phi_{f,0}, \theta_{f,0}) = \{(\pi/4, 3\pi/8), (3\pi/4, \pi/16), (9\pi/8, 3\pi/8), (11\pi/8, \pi/4)\}$. For $r = 1.4$, we see that the ϕ_f and θ_f angles are each dependent on both directions and the angular velocities. We look at the example of

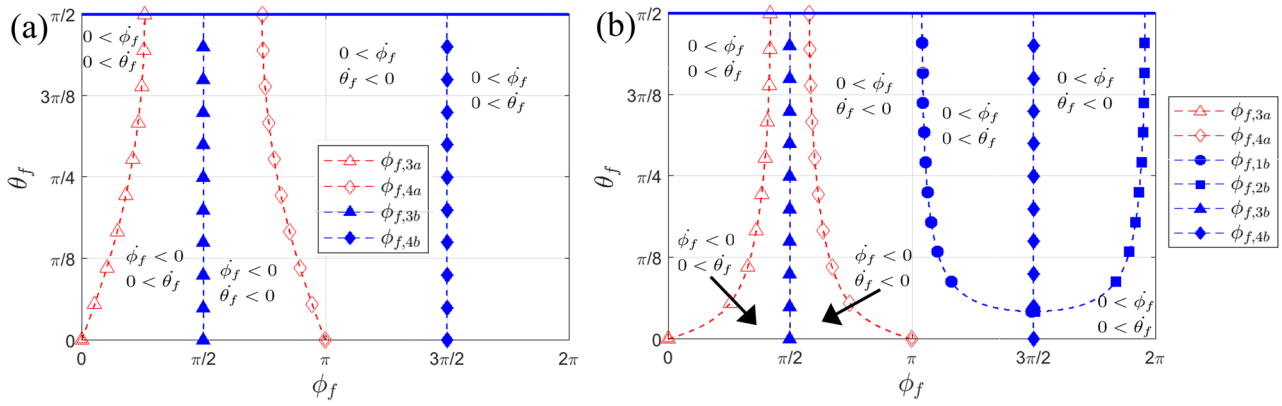

FIG. 4. Particle rotations that affect the particle's angular velocity, $\phi_{f,a}$ and $\phi_{f,b}$, for $\beta = 0$, $S_f = 2$ and for aspect ratios (a) $r = 1.4$ and (b) $r = 4$.

Published under license by AIP Publishing

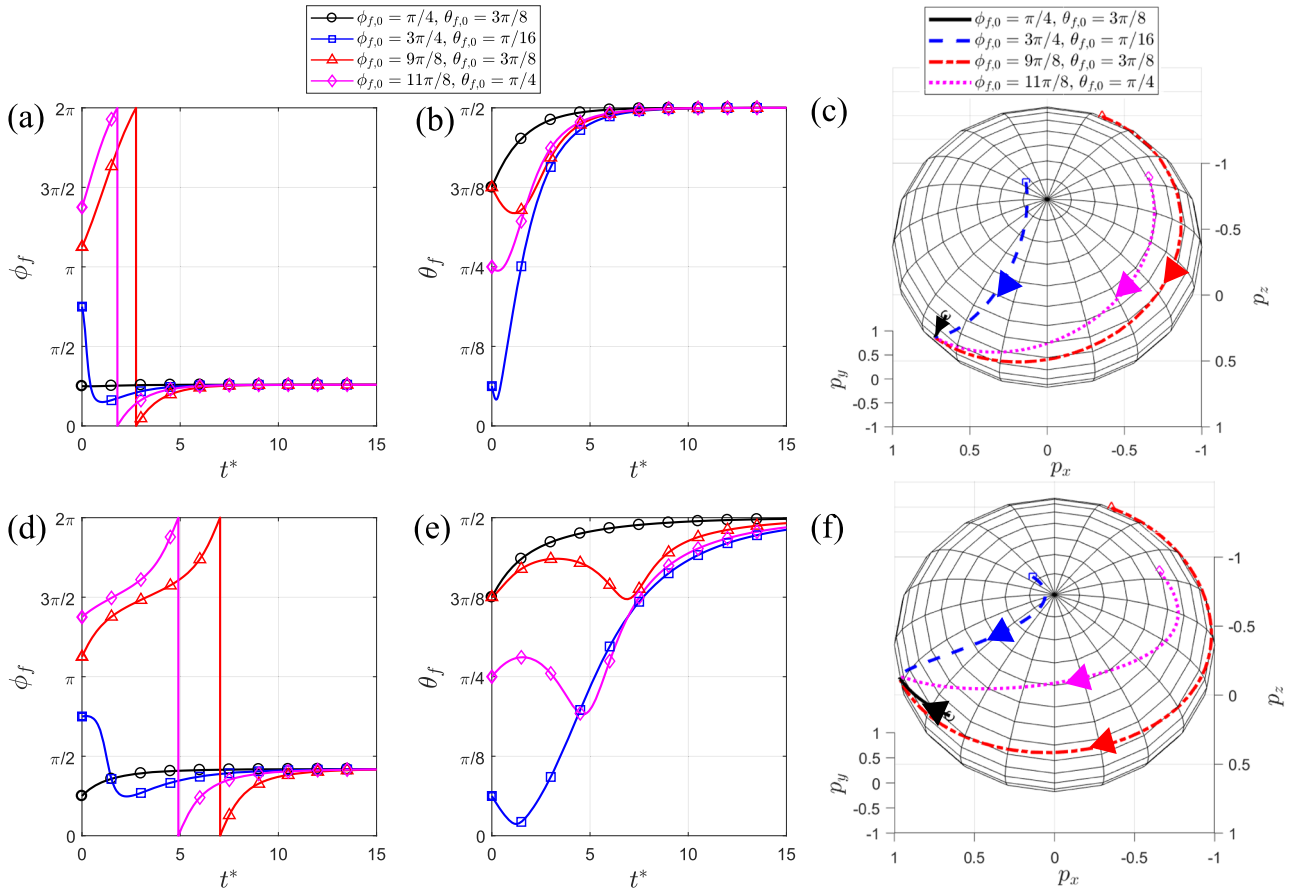

FIG. 5. Time dependent rotation for ϕ_f and θ_f and their trajectories for $\beta = 0$, $S_f = 2$ and for aspect ratios [(a)–(c)] $r = 1.4$ and [(d)–(f)] $r = 4$.

$\phi_{f,0} = 9\pi/8$ and $\theta_{f,0} = 3\pi/8$ which shows that the particle's polar angle θ_f will initially decreases toward zero while the particle's azimuthal angle ϕ_f increases (rotates forwards) toward 2π since $0 < \dot{\phi}_f$ and $\dot{\theta}_f < 0$ are in the range of $\phi_{f,4a} < \phi_f < \phi_{f,4b}$. Then, the particle's polar angle θ_f reaches its trough position at $\phi_f = \phi_{f,4b}$ for the angular velocities $\dot{\phi}_f \neq 0$ and $\dot{\theta}_f = 0$. Afterward, both angular velocities are strictly positive and the particle will rotate toward its stable steady positions $(\phi_f, \theta_f) = (\phi_{f,3a}, \pi/2)$.

We also compare and 4(b), Figs. 5(d), and 5(e) for the same initial angles and for $r = 4$. Initially, the angular velocities are $0 < \dot{\phi}_f$ and $0 < \dot{\theta}_f$ because the initial angles are in the range $\phi_{f,1a} < \phi_f < \phi_{f,4b}$ and $\theta_f(\phi_{f,1b}) < \theta_f < \pi/2$. The particle's polar angle θ_f will reach its peak position at $\phi_f = \phi_{f,4b}$ since $\dot{\theta}_f = 0$ and $0 < \dot{\phi}_f$. Afterward, the particle's polar angle θ_f will decrease toward zero while its azimuthal angle ϕ_f will increase toward 2π since $0 < \dot{\phi}_f$ and $\dot{\theta}_f < 0$ with the time-dependent rotation in the range of $\phi_{f,4b} < \phi_f < \phi_{f,2b}$ and $\theta_f(\phi_{f,2b}) < \theta_f < \pi/2$. When $\phi_f = \phi_{f,2b}$, $\dot{\theta}_f = 0$, and $0 < \dot{\phi}_f$ and $\theta_f(\phi_{f,2b})$ is at the particle's trough for the polar angle θ_f. When $\phi_{f,2b} < \phi_f < \phi_{f,3a}$, $0 < \dot{\phi}_f$ and $0 < \dot{\theta}_f$. Thus, the particle will rotate toward the same stable steady angle as $r = 1.4$.

Figure 5(c) shows a rotation sphere for $r = 1.4$ and Fig. 5(f) for $r = 4$ regarding the initial angles used. Even though the stable steady angles are different for various aspect ratios and strengths, the particles' trajectory may not take the shortest path to the stable steady angle. For initial angles $(\phi_{f,0}, \theta_{f,0}) = \{(3\pi/4, \pi/16), (11\pi/8, \pi/4)\}$, it is obvious the particle's trajectory will curve toward the stable steady angle because the particle's polar angle θ_f will still experience oscillations or experience at least one amplitude. If we want the particle to neither curve nor oscillate (if we want the particle to rotate toward its stable steady angle faster), then S_f would have to be large enough such that $\phi_{f,1b}$ and $\phi_{f,2b}$ do not exist.

When we apply a magnetic field direction at $\beta = \pi$, Figs. 4(a) and 4(b) will experience shifts for our azimuthal angles $\phi_{f,a}$ and $\phi_{f,b}$ and will affect the particles' angular velocities. Compared to $\beta = 0$, the $\phi_{f,a}$-values and $\phi_{f,b}$-values when the magnetic field is applied at $\beta = \pi$ are $\phi_{f,3a} + \pi$ and $\phi_{f,4a} + \pi$, whereas $\phi_{f,1b} - \pi$ and $\phi_{f,2b} - \pi$, respectively. The angles $\phi_{f,3b}$ and $\phi_{f,4b}$ are the same.

2. Parallel to the shear flow $\beta = \pi/2$

For a ferromagnetic particle in a strong field regime parallel to the shear flow, the strength to pin the rotation of the particle is

Published under license by AIP Publishing

$r^2 \leq S_f$ for all aspect ratios. There exists only two steady angles [shown in Figs. 6(a) and 6(b)] with a magnetic field strength of $S_f = r^2 + 1$. For particle aspect ratio $\sqrt{2} < r$, there exists a range of strengths where the ferromagnetic particle can still be pinned when it is initially out of the shear flow and magnetic field plane $2\sqrt{r^2-1} \leq S_f < r^2$. For this range of magnetic field strengths, a particle will either be pinned at its stable steady position or execute periodic rotations. For some initial angles, $\phi_{f,0}$ and $\theta_{f,0}$, there is a range of initial angles that will have the particle orient toward its stable steady position. Shown in Fig. 6(c) are four steady angles (two stable and two unstable) on $\theta_f = \pi/2$ and an out-of-plane critical point on ϕ_f^{cr} and θ_f^{cr} obtained from Eqs. (26) and (27), respectively. Additionally, there are four $\phi_{f,b}$ values to satisfy $\dot{\phi}_f \neq 0$ and $\dot{\theta}_f = 0$.

Figures 6(a) and 7(a)–7(c) represent a ferromagnetic particle with $r = 1.4$ and magnetic field strength $S_f = r^2 + 1$. Since $r^2 - 1 < S_f$, we only have two $\phi_{f,b}$-values: $\phi_{f,3b} = 0$, 2π and $\phi_{f,4b} = \pi$ and two $\phi_{f,a}$-values: $\phi_{f,1a}$ and $\phi_{f,2a}$. The points where both angular velocities are zero are $\theta_f = \pi/2$, $\phi_{f,1a}$ (unstable steady angle) and $\phi_{f,2a}$ (stable steady angle). The time-dependent rotation for ϕ_f in Fig. 7(a) shows that the particle with initial angles greater than the stable steady angle $\phi_{f,0} = 3\pi/4$, $9\pi/8$, and $11\pi/8$ will rotate backward since $\dot{\phi}_f < 0$ is in the range of $\phi_{f,2a} < \phi_f < \phi_{f,1a}$. The initial angle less than the stable steady angle ($\phi_{f,0} = \pi/4$) will rotate forward because $0 < \dot{\phi}_f$ in the range of $\phi_{f,3b} < \phi_f < \phi_{f,2a}$. The time-dependent rotation for θ_f in Fig. 7(b) shows how the particle will rotate based on the initial angles. In the region $\phi_{f,3b} < \phi_f < \phi_{f,4b}$, $0 < \dot{\theta}_f$, and the polar angle θ_f approaches $\pi/2$. In the $\phi_{f,4b} < \phi_f < \phi_{f,3b} = 2\pi$ region, $\dot{\theta}_f < 0$; therefore, the particle will approach its trough at $\phi_{f,3b}$ and $\phi_{f,4b}$ during its rotation toward the stable steady state position, as shown in Fig. 7(b) for initial angles $(\phi_{f,0}, \theta_{f,0}) = \{(9\pi/8, 3\pi/8), (11\pi/8, \pi/4)\}$. As we combine the time-dependent rotations from Figs. 7(a) and 7(b) onto a rotation sphere in Fig. 7(c), we can observe the trajectory of the particle for all initial angles used.

We see similar effects for the aspect ratio $r = 4$ in Figs. 6(b) and 7(d)–7(f) for $S_f = r^2 + 1$. Given that the aspect ratio and the strengths are larger for $r = 4$ than for $r = 1.4$, there will be different values for $\phi_{f,1a}$ and $\phi_{f,2a}$ such that the steady angles are closer to $\pi/2$ and $3\pi/2$, respectively, for this strength. A particle with $r = 4$ will orient toward its stable steady position in a similar manner as $r = 1.4$.

Figures 6(c) and 7(g)–7(i) represent a ferromagnetic particle with $r = 4$, and a magnetic field strength is $S_f = 10$ (in the range $2\sqrt{r^2-1} < S_f < r^2$). Since $S_f < r^2 - 1$, we have four $\phi_{f,a}$-values and four $\phi_{f,b}$-values. In this case, there are four steady angles (two stable and two unstable) on the plane of the magnetic field and one out-of-plane critical angle calculated from Eqs. (26) and (27) (since $S_f = 10 < r^2$) and is a neutrally stable steady angle. At initial angles near the neutrally stable steady angle (i.e., outside the basin of attraction), the particle will complete periodic rotations around the critical point,

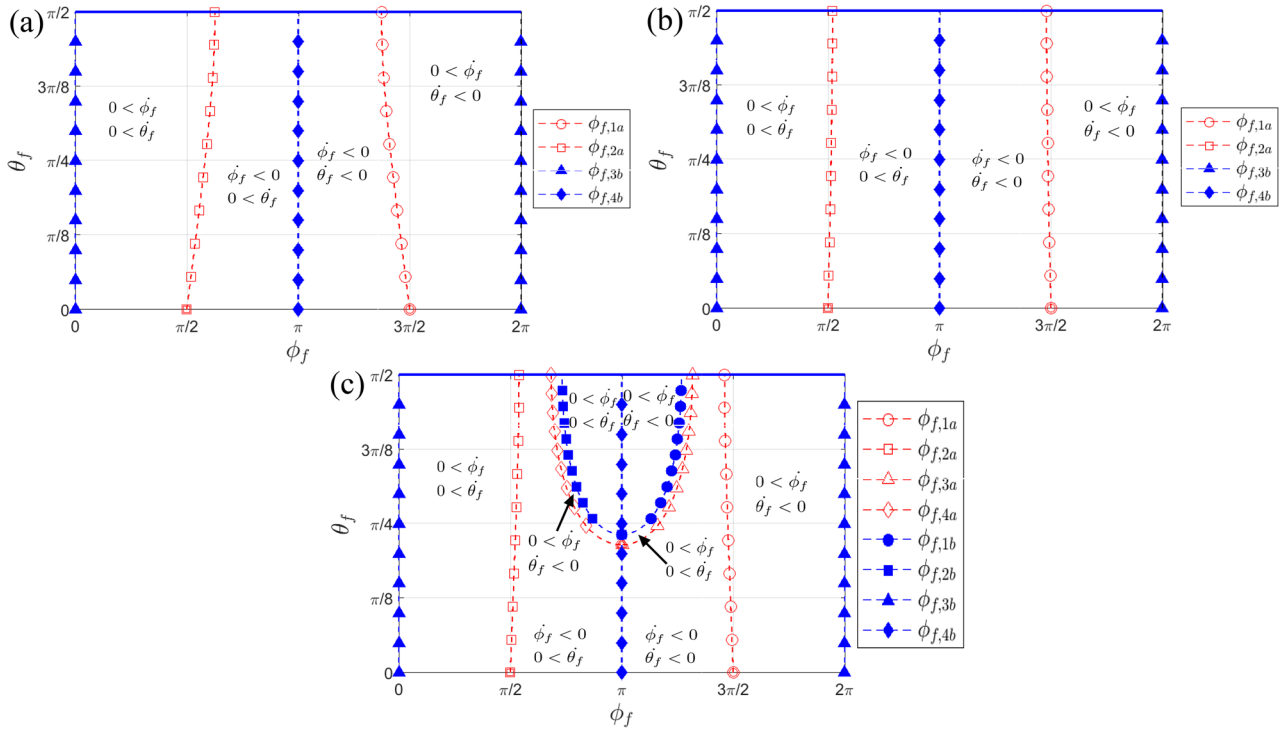

FIG. 6. Particle angular velocity regions described by the particle rotations θ_f, and $\phi_f = \phi_{f,a}$ and $\phi_f = \phi_{f,b}$, for $\beta = \pi/2$ and for (a) $r = 1.4$ and (b) $r = 4$, and for $S_f = r^2 + 1$, and (c) $r = 4$ for $2\sqrt{r^2-1} < S_f = 10 < r^2$.

Published under license by AIP Publishing

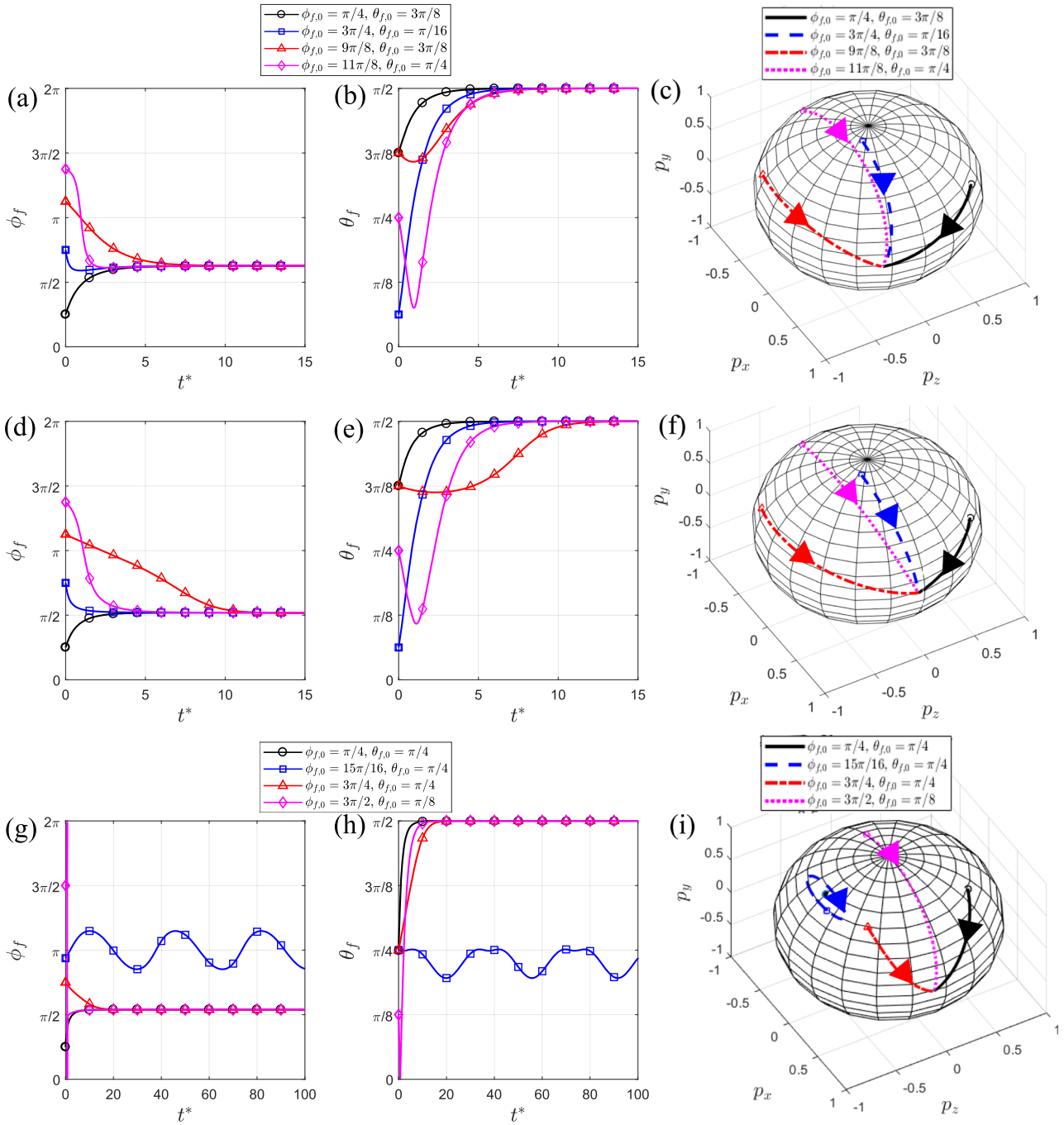

FIG. 7. Time-dependent rotation for ϕ_f and θ_f, for $\beta = \pi/2$, and for aspect ratios [(a)–(c)] $r = 1.4$, [(d)–(f)] $r = 4$ for $S_f = r^2 + 1$, and [(g)–(i)] $r = 4$ and $2\sqrt{r^2 - 1} < S_f = 10 < r^2$.

as shown in Fig. 7(c). In Figs. 7(g) and 7(h), the particle executes periodic oscillations for both ϕ_f and θ_f angles when the initial angles are $\phi_{f,0} = 15\pi/16$ and $\theta_{f,0} = \pi/4$. The amplitudes of the oscillations are both periodic and change for different initial angles. For initial angles inside the basin of attraction and outside the region of $\phi_{f,3a}$ and $\phi_{f,4a}$, the particle will be pinned at a stable steady angle. Given a particle with the initial angles $(\phi_{f,0}, \theta_{f,0}) = \{(\pi/4, \pi/4), (3\pi/4, \pi/4), (3\pi/2, \pi/8)\}$ from Figs. 7(g)–7(i), it will rotate toward $\phi_{2,a}$. Similarly,

Published under license by AIP Publishing

we find that $\phi_{f,1a}$ and $\phi_{f,4a}$ are unstable steady angles, while $\phi_{f,3a}$ is a stable steady angle. The particle will rotate toward $\phi_{f,3a}$ if $\theta_{f,0} = \pi/2$ and $\phi_{f,4a} < \phi_{f,0} < \phi_{f,1a}$.

Compared to $\beta = \pi/2$, the $\phi_{f,a}$-values and $\phi_{f,b}$-values for $\beta = 3\pi/2$ are $\phi_{f,1a} - \pi$ and $\phi_{f,2a} + \pi$ from Figs. 6(a)–6(c), $\phi_{f,3a} - \pi$ and $\phi_{f,4a} + \pi$ from Fig. 6(c), and $\phi_{f,1b} - \pi$ and $\phi_{f,2b} + \pi$ from Fig. 6(c), respectively. The angles $\phi_{f,3b}$ and $\phi_{f,4b}$ are the same.

C. Ferromagnetic particle in a weak magnetic field

In a weak field regime, assuming that the initial angles of a ferromagnetic particle are out-of-plane, it will execute periodic rotations for a magnetic field perpendicular and parallel to the shear flow. The eigenvalues for ϕ_f^{cr} and θ_f^{cr} are therefore neutrally stable, and a ferromagnetic particle will perform periodic rotations around the critical point. For certain initial angles, there exists an orbital region in which ϕ_f will not execute periodic rotations (i.e., ϕ_f will oscillate) and θ_f will conduct periodic oscillations with one amplitude for $\beta = 0$ or two amplitudes for $\beta = \pi/2$. For all aspect ratios, when $\beta = 0$, there exists two $\phi_{f,a}$-values and four $\phi_{f,b}$-values. For $\beta = \pi/2$, an aspect ratio of $1 < r \le \sqrt{2}$ will have two $\phi_{f,a}$-values, while aspect ratios $\sqrt{2} < r$ will have four $\phi_{f,a}$-values; there exists four $\phi_{f,b}$-values for all aspect ratios.

1. Parallel to the velocity field gradient $\beta = 0$

A magnetic field applied perpendicular to the shear flow is expressed as a weak magnetic field when $S_f < 1$ for all aspect ratios. Shown in Fig. 8 are the angular velocity effects for our azimuthal angles $\phi_{f,a}$ and $\phi_{f,b}$, for (a) $r = 1.4$ and (b) $r = 4$ and for the magnetic field strength $S_f = 0.5$. For $\beta = 0$ and for $1 < r$, the critical angles are $\phi_f^{cr} = \pi/2$ and $\theta_f^{cr} = \arcsin(S_f)$. The curves for $\phi_{f,3a}$ and $\phi_{f,4a}$ will otherwise become different for each aspect ratio; each aspect ratio will affect the time-dependent periodic rotation of the particle seen in Fig. 9 even when each particles' initial angles are the same. The periodic rotation around the critical point will become different as seen in Figs. 9(c) and 9(f). For the aspect ratio $r = 4$, the path of the rotation around the critical point becomes more elliptic and the amplitudes in Fig. 9(e) differ greatly for $\phi_{f,0} = 3\pi/4$ and $\theta_{f,0} = \pi/16$. The time to complete a periodic rotation becomes longer than for $r = 1.4$. We make additional observations for Figs. 9(a) and 9(b) for $r = 1.4$ that particles with initial angles $(\phi_{f,0}, \theta_{f,0}) = \{(\pi/4, 3\pi/8), (9\pi/8, 3\pi/8), (11\pi/8, \pi/4)\}$ will experience oscillations for the polar angle θ_f and periodic rotations for the azimuthal angle ϕ_f. Since they perform periodic rotations, the particles' rotation will experience two amplitudes for θ_f during their time dependent rotation. For the initial angles $\phi_{f,0} = 3\pi/4$ and $\theta_{f,0} = \pi/16$, the particles' azimuthal angle ϕ_f will execute periodic oscillations as well as for the polar angle θ_f. By using our numerical analysis, the particles will not rotate around the zenith of the sphere seen in Fig. 9(c) but will instead rotate around the critical point. One observation is that the particles are initially in the region $\phi_{f,3a} < \phi_f < \phi_{f,4a}$ and $0 < \theta_f < \theta_f^{cr}$ and will encircle around the critical point since there exists only one constant amplitude. Further observations can be made for $r = 4$. For all of the particles' initial angles, they are outside the region of orbit because the particles will complete periodic rotations and have two constant amplitudes. Therefore, we can conclude that for this magnetic field direction and strength, as long as the initial rotations are outside the region of orbit, the particles will execute periodic rotations for its azimuthal angle ϕ_f. Figures 9(c) and 9(f) shows a rotation sphere for $r = 1.4$ and $r = 4$, respectively.

Compared to $\beta = 0$, the $\phi_{f,a}$ and $\phi_{f,b}$-values for $\beta = \pi$ are $\phi_{f,3a} + \pi$ and $\phi_{f,4a} + \pi$, and $\phi_{f,1b} - \pi$ and $\phi_{f,2b} - \pi$, respectively. The angles $\phi_{f,3b}$ and $\phi_{f,4b}$ are the same.

2. Parallel to the shear rate $\beta = \pi/2$

For a magnetic field parallel to the shear flow, a particle is in weak field regime when $S_f < r^2$ for aspect ratios $1 < r \le \sqrt{2}$ and $S_f < 2\sqrt{r^2 - 1}$ for aspect ratios $\sqrt{2} < r$. Figure 10 shows the angular velocity effects for the azimuthal angles $\phi_{f,a}$ and $\phi_{f,b}$ when (a) $r = 1.4$ and (b) $r = 4$ with a magnetic field strength $S_f = 5$. For $\beta = \pi/2$ and for all aspect ratios, the critical angles are $\phi_f^{cr} = \pi$ and $\theta_f^{cr} = \arcsin(S_f/r^2)$. For all aspect ratios, there exists four $\phi_{f,b}$-values. For $1 < r \le \sqrt{2}$, there exists two $\phi_{f,a}$-values, $\phi_{f,1a}$ and $\phi_{f,2a}$, while $\sqrt{2} < r$ has four $\phi_{f,a}$-values. Similar to the magnetic field perpendicular to the shear flow, the particle's rotation will be affected by the magnetic field strength, the particle aspect ratio, and the initial directions.

For a particle aspect ratio $r = 1.4$, the ϕ_{f1b}-curves and ϕ_{f2b}-curves converge closer to $\pi/2$ as the strength approaches to its critical

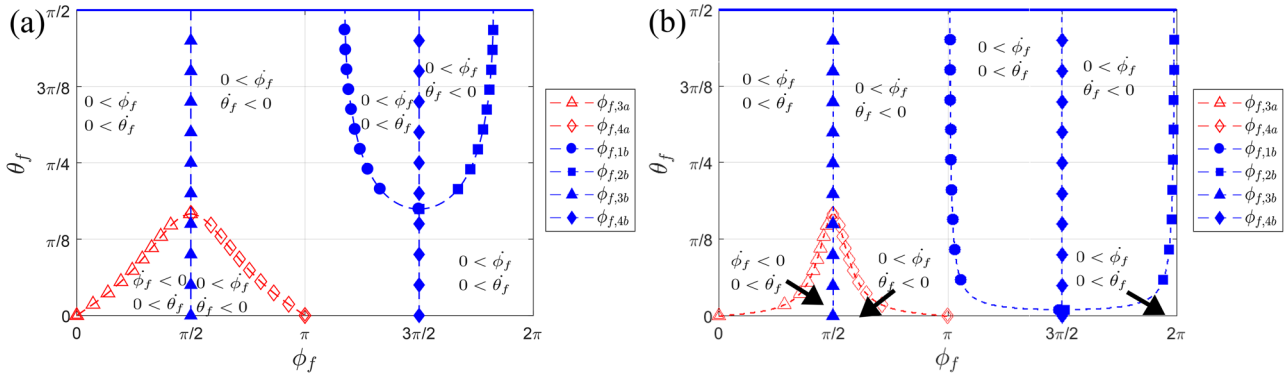

FIG. 8. Particle angular velocity regions described by the particle rotations θ_f, and $\phi_f = \phi_{f,a}$ and $\phi_f = \phi_{f,b}$, for $\beta = 0$, for $S_f = 0.5$, and for aspect ratios (a) $r = 1.4$ and (b) $r = 4$.

Published under license by AIP Publishing

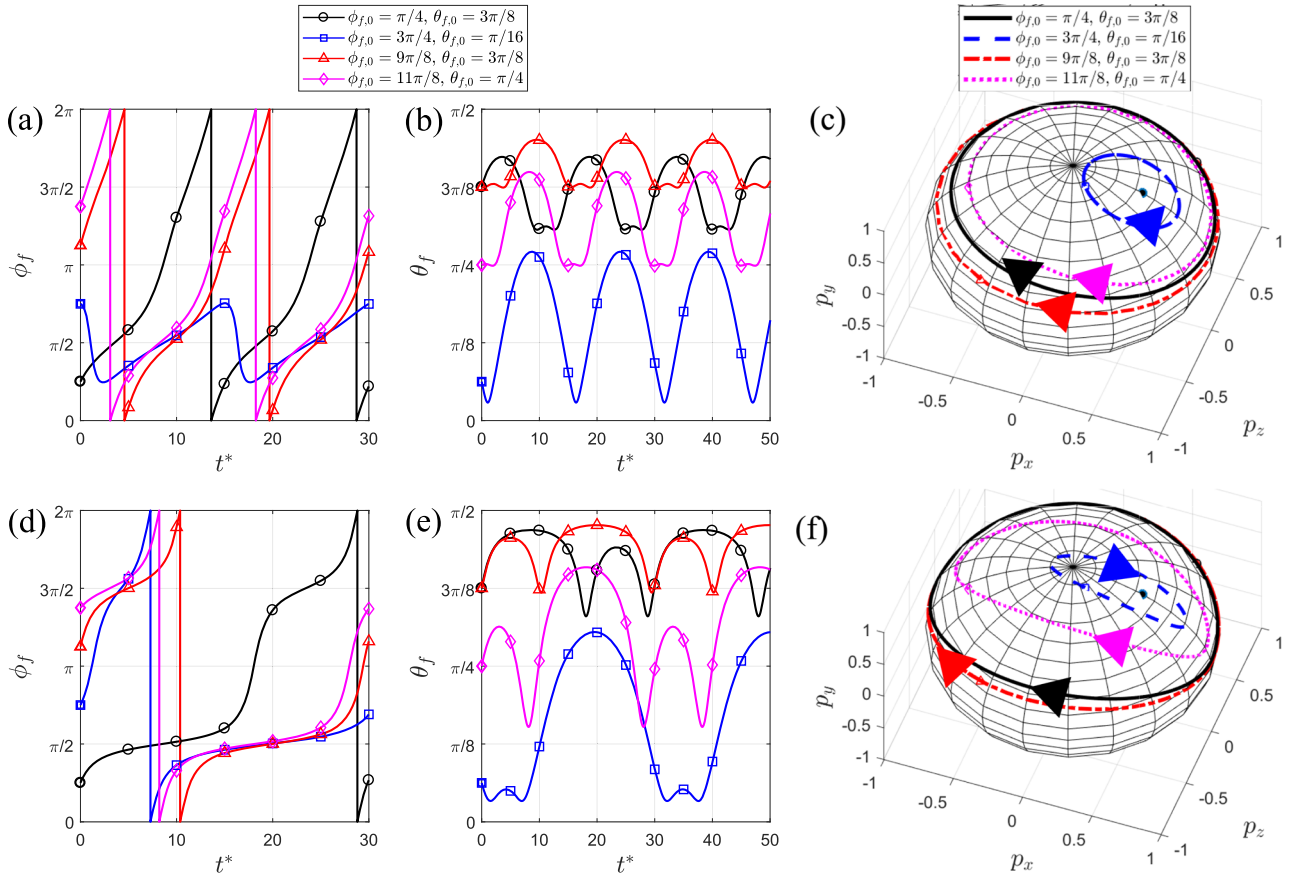

FIG. 9. Time-dependent rotation for ϕ_f and θ_f, and their trajectories for $\beta = 0$, $S = 0.5$, and for aspect ratios [(a)–(c)] $r = 1.4$ and [(d)–(f)] $r = 4$.

strength. For the magnetic field strength $S_f = 0.5$ and for initial angles $\phi_{f,0} = 3\pi/4$ and $\theta_{f,0} = \pi/16$, the particle will be in the region of orbit and therefore ϕ_f will not complete a full periodic rotation and θ_f will experience only one amplitude. Other initial angles used in this example are outside the region of orbit, so ϕ_f will execute periodic rotations and θ_f will execute two periodic amplitudes with their range of their oscillations varying with the angular velocities that the particle will experience.

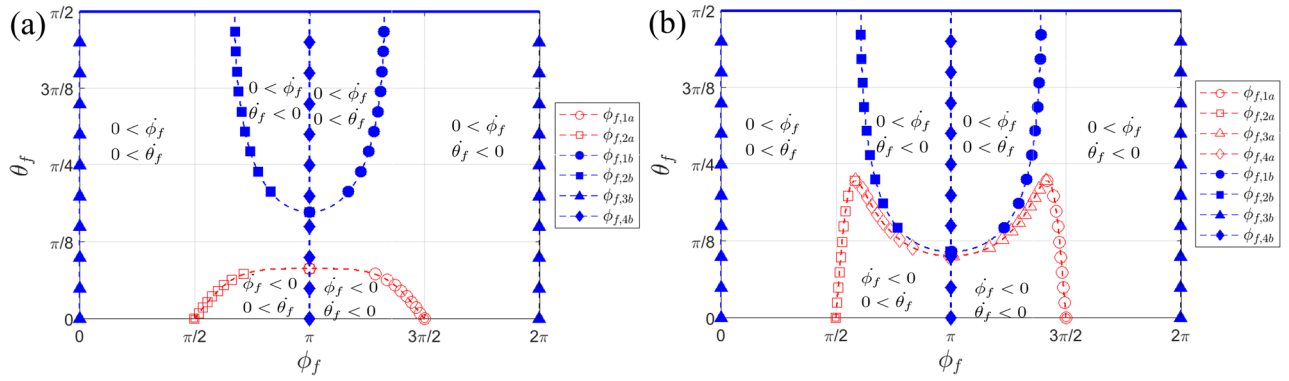

FIG. 10. Particle angular velocity regions described by the particle rotations θ_f, and $\phi_f = \phi_{f,a}$ and $\phi_f = \phi_{f,b}$, $\beta = \pi/2$, and for aspect ratios and strengths (a) $r = 1.4$ for $S_f = 0.5$ and (b) $r = 4$ for $S_f = 5$.

Published under license by AIP Publishing

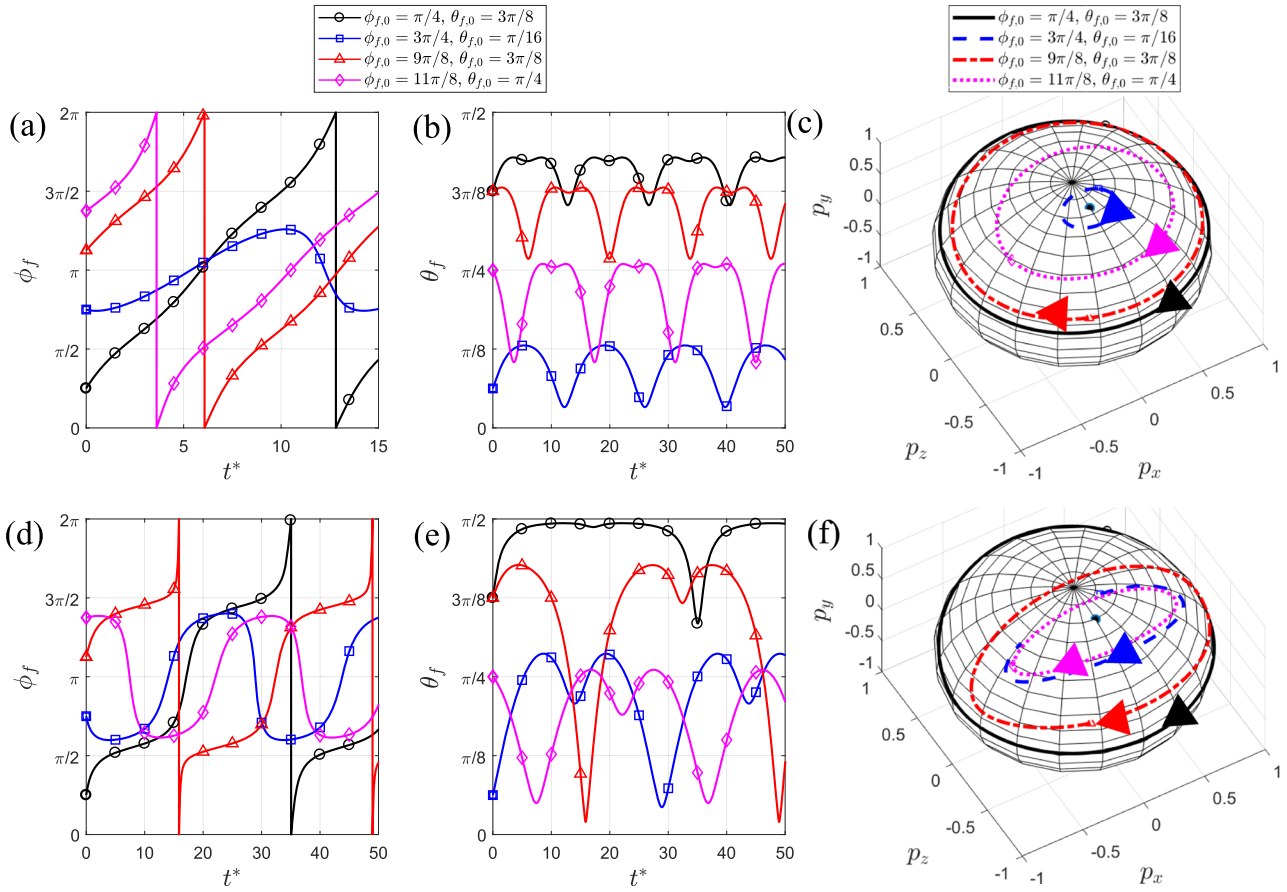

FIG. 11. Time dependent rotation for ϕ_f and θ_f, and trajectories for $\beta = \pi/2$, and for aspect ratios [(a)–(c)] $r = 1.4$ for $S_f = 0.5$ and [(d)–(f)] $r = 4$ for $S_f = 5$.

The rotation spheres in Figs. 11(c) and 11(f) shows that for some aspect ratios, the initial angles will be in the region of orbit since the trajectory of the particle will not encircle the zenith of the sphere. The effects of the path of the particle and initial rotations from Fig. 11 indicate that for the aspect ratio $r = 4$ and initial angles $(\phi_{f,0}, \theta_{f,0}) = \{(3\pi/4, \pi/16), (11\pi/8, \pi/4)\}$ in (d) the azimuthal angle ϕ_f will oscillate between $\pi/2$ and $3\pi/2$ and the polar angle θ_f will oscillate between 0 and $3\pi/8$ in (e). Unlike a magnetic field perpendicular to the shear flow, a particle in this example will have two periodic amplitudes since ϕ_f approaches ϕ_{f1b}, ϕ_{f2b}, and ϕ_{f4b} although it may still be possible to have one amplitude if the initial rotations are very close to the critical point. Since the other initial rotations are outside of the region of orbit, the particle will execute periodic rotations and their amplitudes will vary depending on the angular velocities throughout the time dependent rotation.

Compared to $\beta = \frac{\pi}{2}$, the $\phi_{f,a}$- and $\phi_{f,b}$-values for $\beta = 3\pi/2$ depend on the aspect ratio. For $r = 1.4$ and $S_f = 0.5$, the $\phi_{f,a}$-values are $\phi_{f,1a} - \pi$ and $\phi_{f,2a} + \pi$, and for $r = 4$ and $S_f = 5$, the values are $\phi_{f,1a} - \pi$, $\phi_{f,2a} + \pi$, $\phi_{f,3a} - \pi$, and $\phi_{f,4a} + \pi$. For both aspect ratios, the $\phi_{f,b}$-values are $\phi_{f,1b} - \pi$ and $\phi_{f,2b} + \pi$, but the angles $\phi_{f,3b}$ and $\phi_{f,4b}$ are the same.

VII. CONCLUSION

We investigated a time-dependent, three-dimensional rotation regarding paramagnetic and ferromagnetic ellipsoidal particles in simple shear flows and in a uniform magnetic field. We analyzed, analytically and numerically, the rotations of the particles due to the magnetic field and determined the critical field strengths and directions. For paramagnetic particles exposed to a magnetic field at or above its critical field strength, we determined the critical/stable steady angle. Two coupled ordinary differential equations describing the time evolution of the particles' rotation were analyzed from its initial angle to its stable steady angle. If the magnetic field strength is less than the critical, a paramagnetic particle will oscillate toward the magnetic field plane and will continue to execute periodic rotations. We found the analytical equations that determine the maximum and minimum of θ_p during the periodic rotation. By knowing what the peaks and troughs are, we can

Published under license by AIP Publishing

determine the amplitudes. The magnetic field strengths and directions will determine the number of oscillations that the particle will experience.

For a ferromagnetic particle, the critical angle's stability can be determined by analyzing the eigenvalues calculated from the Lyaponov theorem in spherical coordinates. If the magnetic field strength is greater than the critical field strength, the ferromagnetic particle's rotation will be pinned at a stable steady angle and lie in the magnetic field plane. When a magnetic field is applied perpendicular to the vorticity but is either parallel or perpendicular to the simple shear flow, the ferromagnetic particle will impede at a stable steady angle. For a magnetic field parallel to the simple shear flow and for a certain particle aspect ratio, we determined that there exists a range of magnetic field strengths for a particle to rotate toward a stable steady angle. If, however, the initial angles of the particle are outside a certain range, the ferromagnetic particle will execute periodic rotations around the critical angle. When the magnetic field strength is less than the critical field strength, the ferromagnetic particle will execute periodic rotations around the critical angle, but whether the particle's azimuthal angle ϕ_f will execute complete rotations or oscillate is numerically determined.

For both strong and weak magnetic field strengths, we determined multiple analytic equations that found the directions of the ferromagnetic particle and causes one of the angular velocities equal to zero. These equations can determine the peaks and troughs of the ferromagnetic particle's rotation. To analyze the time-dependent rotations for our ϕ_f and θ_f angles, we use our numerical analysis to determine the peaks, troughs, and amplitudes and analyzed the behavior of the particle in weak and strong magnetic field regimes. As we will see in the Appendix, if the magnetic particle is placed in an arbitrary direction, the particle will either oscillate to the same plane as the magnetic field and perform periodic rotations or oscillate and be pinned at a critical angle.

Given our analyses on the rotational dynamic differences between paramagnetic and ferromagnetic particles, our work can greatly offer a key to efficiently separate magnetic materials or deliver drugs without using a magnetic force. If we apply a magnetic field strength at an arbitrary direction, we notice that S_p and S_f are unique and will affect their respected angles ϕ_p, θ_p, ϕ_f, and θ_f. Since their critical strengths differ, for each magnetic field direction and particle aspect ratio, a magnetic field strength may result in $S_f^{cr} < S_f$ but $S_p < S_p^{cr}$ and vise-versa. Analyzing their angular velocities and pinned directions can assist in separations since a ferromagnetic particle may have its rotational dynamics pinned out of the magnetic field plane, whereas a paramagnetic particle will always either be pinned or execute periodic rotations on the magnetic field plane. If both particles lie on the magnetic field plane, their stable steady directions and angular velocities can identify what type of magnetic particles we are observing.

By further analyzing their time-dependent rotations, we can predict their migration behaviors in rectangular channels. In this case, the migration of the particle will depend on its rotational dynamics and the particle-wall interaction. In two-dimensional cases, previous authors used a dimensionless variable, τ, as a ratio between the amount of time the particle spends in the first half of its rotation (ϕ from 0 to $\pi/2$) with the time it spends in a full rotation (ϕ from 0 to π).[11,12,14] Accordingly, a particle in the absence of a magnetic field will oscillate, but it does not experience a net migration after one periodic rotation because the rotation is symmetric ($\tau = 0.5$). When a magnetic field is applied, the symmetry of rotation is broken. If $\tau < 0.5$, the result is a migration toward the channel wall. When $\tau > 0.5$, the particle will migrate away from the channel wall. When the magnetic field is strong enough to pin the particle at a stable steady angle, the particle will have a net migration toward or away from the wall without any oscillations. In these cases, we saw that the paramagnetic and ferromagnetic particles had different τ values such that separation between the two is feasible.[12] Matsunaga *et al.* discussed the dynamics of a ferromagnetic particle in a rectangular channel and under a two-dimension magnetic field that pins the particle at a stable steady angle (Ref. 13). Research evaluations considering the particle's rotation in a rectangular channel and under a weak magnetic field are still missing. While we touched on a deeper understanding regarding the comparison between paramagnetic and ferromagnetic particles, it would be beneficial for these particles to be studied. By using our theoretical analysis from this and previous articles, we can apply a particle's rotational dynamics in an unbounded fluid domain to a particle in a closed rectangular channel using the far-field theory from Matsunaga *et al.*, and thus, attempt to predict the particle's dynamics.

Even though we studied these particles separately, an effective separation/deliverance can occur when a concentration of particles is diluted enough to prevent particle-particle interactions. These rotational dynamics can assist as a cost effective separation of paramagnetic or ferromagnetic ellipsoidal particles and identify elements in mining explorations instead of using expensive machinery. Applying magnetic fields can be used as an innovative filtration system to extract harmful metals in public water treatment facilities instead of relying solely on hydrodynamic effects.

ACKNOWLEDGMENTS

The first author gratefully acknowledges the financial support from the Chancellor's Distinguished Fellowship at Missouri University of Science and Technology (to C.A.S.).

APPENDIX: FERROMAGNETIC PARTICLE: $\beta = \pi/4$ AND $\beta = 3\pi/4$

For a magnetic field direction at $\beta = \pi/4$ ($\beta = 5\pi/4$), the particle will rotate toward its stable steady position for the strong field regime $\left(\frac{r^2}{\sqrt{\sin^2(\beta) - r^4\cos^2(\beta)}} < S_f\right)$. In a strong field regime, we assume that $\theta_f = \pi/2$ and we use Eq. (31) to find the stable steady angles. Shown in Fig. 12 are two $\phi_{f,a}$-values, $\phi_{f,3a}$ and $\phi_{f,4a}$, for both $r = 1.4$ in (a) and $r = 4$ in (b). For $r = 1.4$, there are two $\phi_{f,b}$-values, $\phi_{f,1b}$ and $\phi_{f,2b}$, and four $\phi_{f,b}$-values for $r = 4$. In both cases, the stable steady angles are $\theta_f = \pi/2$ and $\phi_{f,3a}$, while $\phi_{f,4a}$ is an unstable steady stable angle. Therefore, by comparing Figs. 12 and 13, we can determine how the particle will behave as it rotates toward its stable steady position. Furthermore, we see the trajectory of the particle for $r = 1.4$ in Fig. 13(c) and for $r = 4$ in Fig. 13(f). Given the initial rotations, the magnetic field strengths, and the aspect ratios, we can therefore observe the trajectory of the particle for theoretical and numerical studies. For the initial rotations $(\phi_{f,0}, \theta_{f,0}) = \{(9\pi/8, 3\pi/8),$

Published under license by AIP Publishing

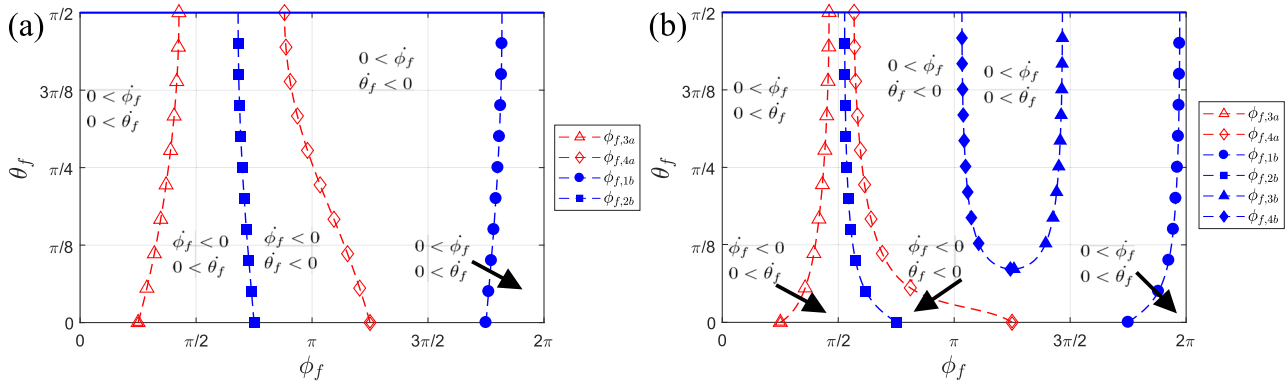

FIG. 12. Particle angular velocity regions described by the particle rotations θ_f, and $\phi_f = \phi_{f,a}$ and $\phi_f = \phi_{f,b}$, for $\beta = \pi/4$, $S_f = 2$, and for aspect ratios (a) $r = 1.4$ and (b) $r = 4$.

$(11\pi/8, \pi/4)\}$, the ferromagnetic particle, for both aspect ratios, will curve around the zenith of the rotation sphere, while the initial rotation $\phi_{f,0} = 3\pi/4$ and $\theta_{f,0} = \pi/16$ will curve toward the zenith and then approach the stable steady angle.

For a magnetic field strength $S_f < \frac{r^2}{\sqrt{\sin^2(\beta)+r^4\cos^2(\beta)}}$, we can identify that from Eq. (25) that the real part of the eigenvalues will become positive. Therefore, ϕ_f^{cr} and θ_f^{cr} are unstable angles and the particle will oscillate toward $\theta_f = \pi/2$ and where ϕ_f will continue

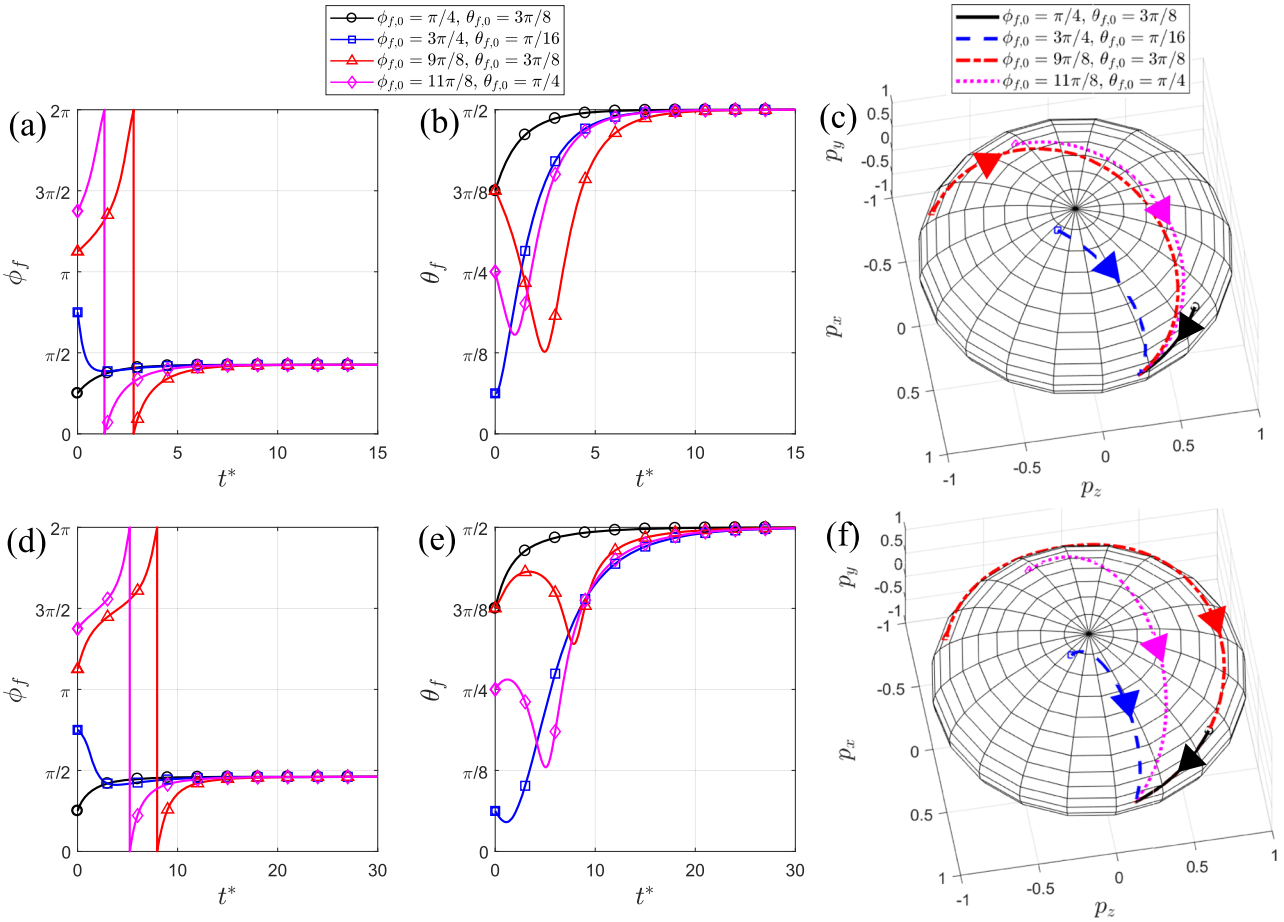

FIG. 13. Time dependent rotation for ϕ_f and θ_f and their trajectories for $\beta = \pi/4$, $S_f = 2$, and for aspect ratios [(a)–(c)] $r = 1.4$ and [(d)–(f)] $r = 4$.

Published under license by AIP Publishing

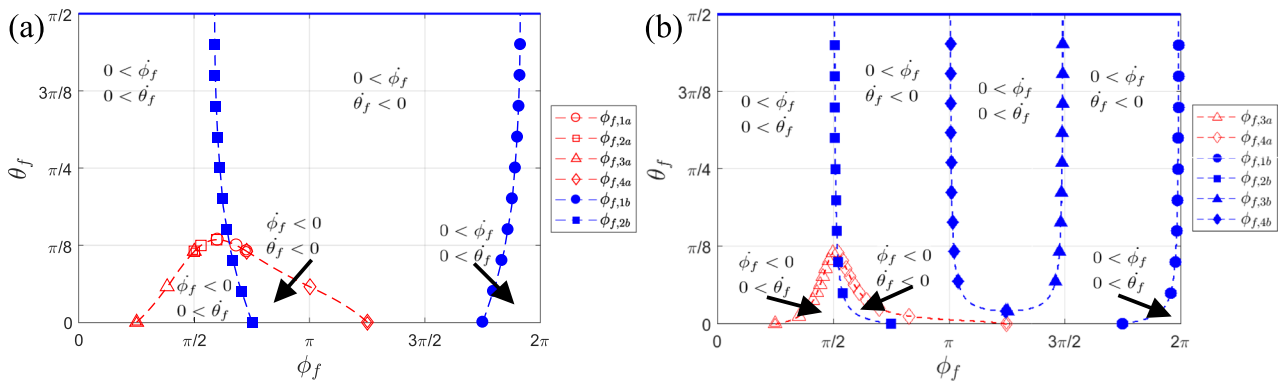

FIG. 14. Particle angular velocity regions described by the particle rotations θ_f, and $\phi_f = \phi_{f,a}$ and $\phi_f = \phi_{f,b}$, for $\beta = \pi/4$, $S_f = 0.5$, and for aspect ratios (a) $r = 1.4$ and (b) $r = 4$.

to execute periodic rotations. Shown in Fig. 14 are four $\phi_{f,a}$-values for $r = 1.4$ in (a) and two $\phi_{f,a}$-values, $\phi_{f,3a}$ and $\phi_{f,4a}$, for $r = 4$ in (b). For $r = 1.4$, there are two $\phi_{f,b}$-values, $\phi_{f,1b}$ and $\phi_{f,2b}$, and four $\phi_{f,b}$-values for $r = 4$. In both cases, the ferromagnetic particle will conduct oscillations and rotations. Unlike the paramagnetic particle, the angular velocities for the ferromagnetic particle depend on both angular directions. Therefore, the particle's ϕ_f periodic rotation will constantly change as θ_f approaches toward $\pi/2$. Figure 15 shows the rotation of a ferromagnetic particle for [(a)–(c)] $r = 1.4$ and for [(d)–(f)] $r = 4$ and for the magnetic field strength $S_f = 0.5$. We observe that a particle with aspect ratio $r = 1.4$ will oscillate faster to the same plane than the aspect ratio $r = 4$ because the strength to

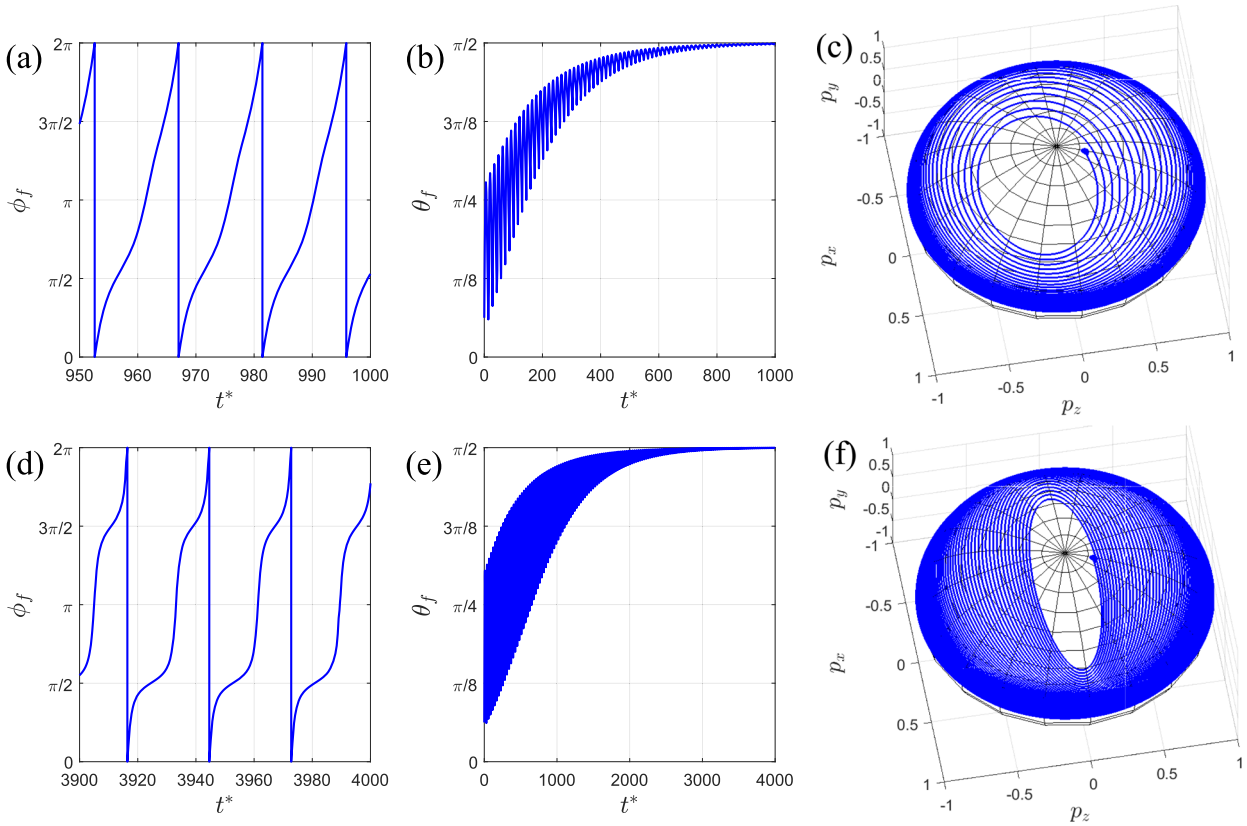

FIG. 15. Time dependent rotation for ϕ_f and θ_f, and their trajectories for $\beta = \pi/4$, $S_f = 0.5$, and for aspect ratios [(a)–(c)] $r = 1.4$ and [(d)–(f)] $r = 4$.

Published under license by AIP Publishing

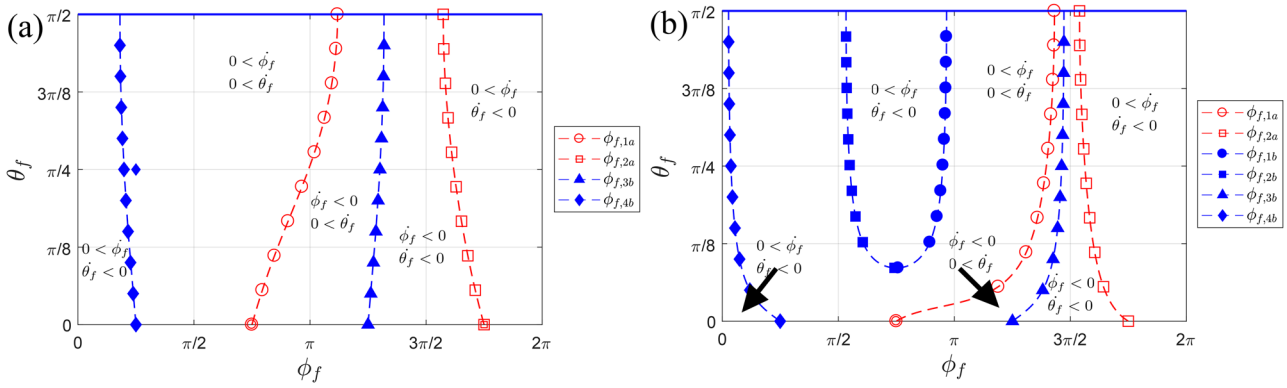

FIG. 16. Particle angular velocity regions described by the particle rotations θ_f, and $\phi_f = \phi_{f,a}$ and $\phi_f = \phi_{f,b}$, for $\beta = 3\pi/4$, $S_f = 2$, and for aspect ratios (a) $r = 1.4$ and (b) $r = 4$.

impede the particle in magnetic field plane, $S_f = \frac{r^2}{\sqrt{\sin^2(\beta)+r^4\cos^2(\beta)}}$, is greater as the aspect ratio increases. Consequentially, the rotation of the particle will slowly approach toward the magnetic field plane. Furthermore, we see the trajectory of the particle for $r = 1.4$ in Fig. 15(c) and for $r = 4$ in Fig. 15(f). Given the initial angles, the magnetic field strengths, and the aspect ratios, we observe the trajectory of the particle given the theoretical and numerical studies where the ferromagnetic particle for $r = 1.4$ will rotate around the sphere less than for $r = 4$. For $r = 4$, the rotation of the particle initially has a larger elliptic shape around the zenith and converges to a circular rotation around the sphere at $\theta_f = \pi/2$.

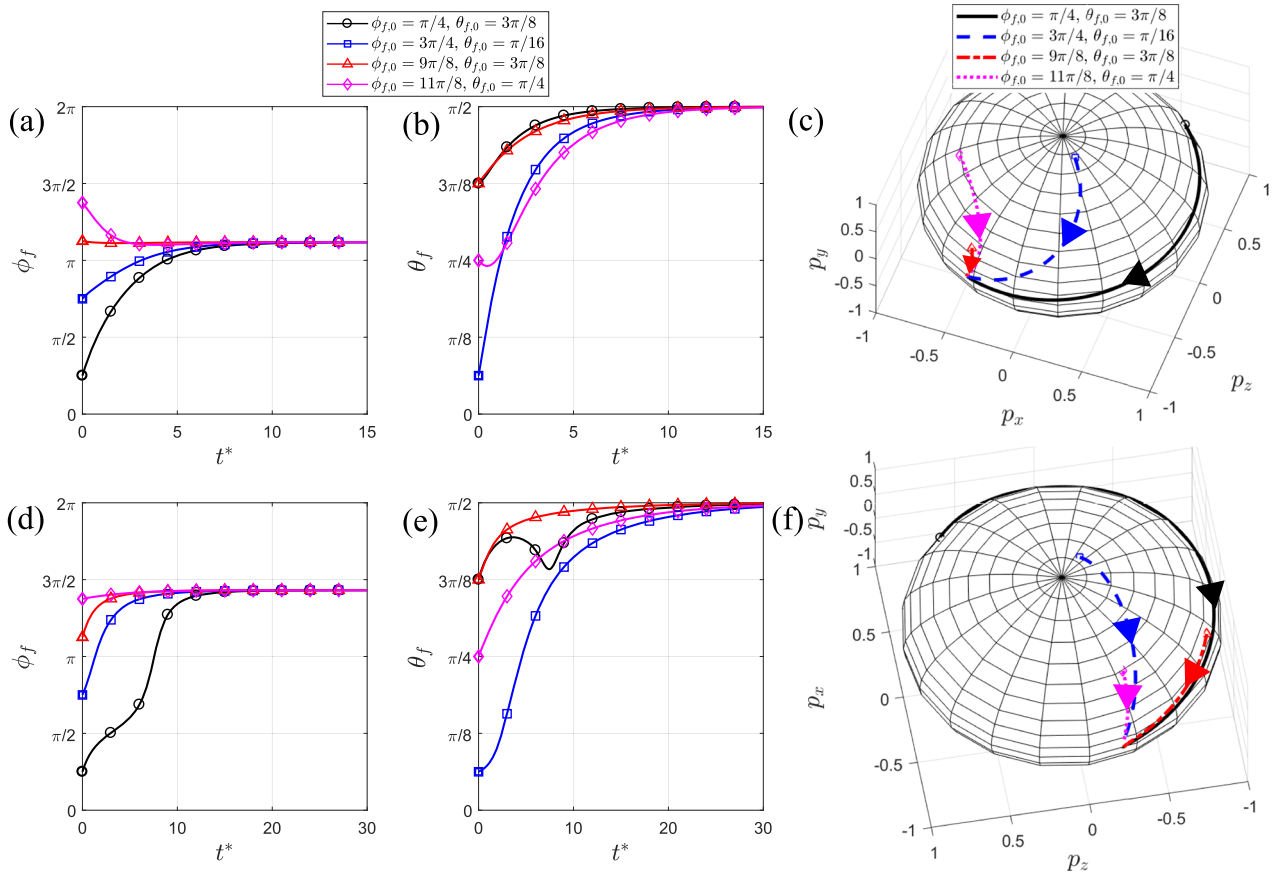

FIG. 17. Time-dependent rotation for ϕ_f and θ_f, and their trajectories for $\beta = 3\pi/4$, $S_f = 2$, and for aspect ratios [(a)–(c)] $r = 1.4$ and [(d)–(f)] $r = 4$.

Published under license by AIP Publishing

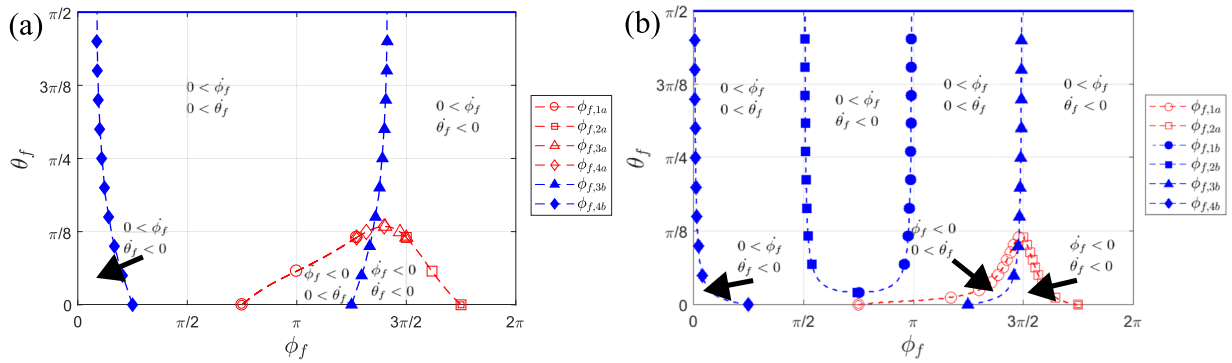

FIG. 18. Particle angular velocity regions described by the particle rotations θ_f, and $\phi_f = \phi_{f,a}$ and $\phi_f = \phi_{f,b}$, for $\beta = 3\pi/4$, $S_f = 0.5$, and for aspect ratios (a) $r = 1.4$ and (b) $r = 4$.

For magnetic field directions $\beta = 3\pi/4$ ($\beta = 7\pi/4$), the particle will rotation toward its stable steady position in a strong field regime or will oscillate toward its stable steady critical angle ϕ_f^{cr} and θ_f^{cr} obtained from Eqs. (26) and (27) because the eigenvalues are negative. For a particle in a strong field regime, $\frac{r^2}{\sqrt{\sin^2(\beta) - r^4\cos^2(\beta)}} < S_f$, $\theta = \pi/2$, and use Eq. (31) to find the stable steady angles. Shown in Fig. 16, there exists two $\phi_{f,a}$-values, $\phi_{f,1a}$ and $\phi_{f,2a}$, for both $r = 1.4$ in (a) and $r = 4$ in (b). For $r = 1.4$, there are

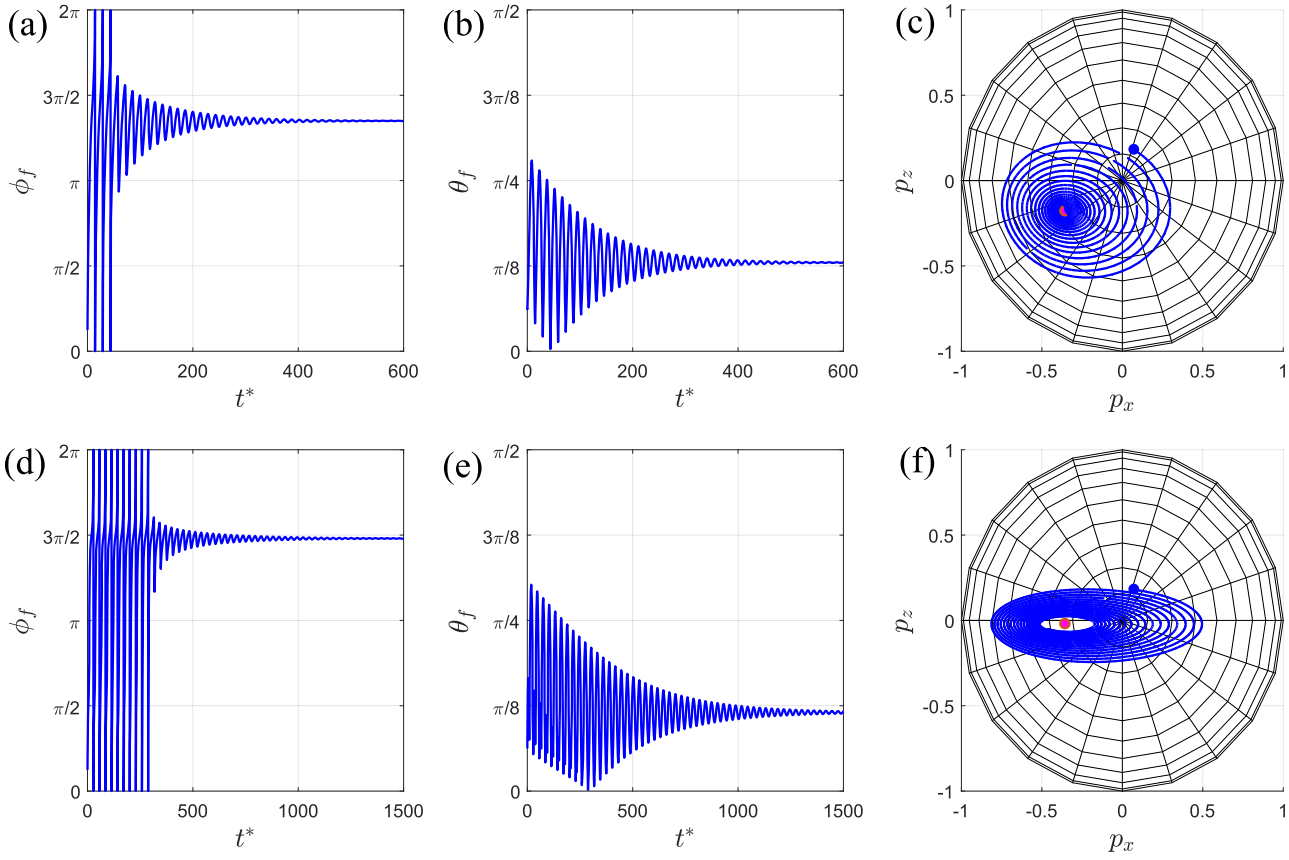

FIG. 19. Time dependent rotation for ϕ_f and θ_f, and their trajectories for $\beta = 3\pi/4$, $S_f = 0.5$, and for aspect ratios [(a)–(c)] $r = 1.4$ and [(d)–(f)] $r = 4$.

Published under license by AIP Publishing

two $\phi_{f,b}$-values, $\phi_{f,3b}$ and $\phi_{f,4b}$, and four $\phi_{f,b}$-values for $r = 4$. In both cases, the stable steady angles are $\theta_f = \pi/2$ and $\phi_{f,1a}$, while $\phi_{f,2a}$ is an unstable steady stable angle. Therefore, by comparing Figs. 16 and 17, we can determine how the particle will behave as it rotates toward its stable steady position. Furthermore, we see the trajectory of the particle for $r = 1.4$ in Fig. 17(c) and for $r = 4$ in Fig. 17(f). Given the initial angles, the magnetic field strengths, and the aspect ratios, we can therefore observe the trajectory of the particle given the theoretical and numerical studies. For the same initial angles as we used for the magnetic field direction $\beta = \pi/4$, the ferromagnetic particle, for both aspect ratios, will curve toward that stable steady angle.

For a magnetic field strength $0 < S_f < \frac{r^2}{\sqrt{\sin^2(\beta) - r^4\cos^2(\beta)}}$, an evaluation from Eq. (25) states that the real part of the eigenvalues are negative. Thus, ϕ_f^{cr} and θ_f^{cr} are stable angles and the particle will oscillate toward the critical angles. In Fig. 18, there exists four $\phi_{f,a}$ values for $r = 1.4$ in (a) and two $\phi_{f,a}$-values, $\phi_{f,1a}$ and $\phi_{f,2a}$, for $r = 4$ in (b), two $\phi_{f,b}$-values, $\phi_{f,3b}$ and $\phi_{f,4b}$, for $r = 1.4$, and four $\phi_{f,b}$-values for $r = 4$. Figure 19 shows the oscillation of a ferromagnetic particle toward the stable critical angles for [(a)–(c)] $r = 1.4$ and for [(d)–(f)] $r = 4$ and for the magnetic field strength $S_f = 2$. We observe that larger particle aspect ratios will oscillate slower toward their critical angles. We also observe the trajectory of the particle for $r = 1.4$ in Fig. 19(c) and for $r = 4$ in Fig. 19(f). Given the initial angles, the magnetic field strengths, and the aspect ratios and observing the trajectory of the particle given the theoretical and numerical studies, the ferromagnetic particle will spiral toward the critical angle. The shape of the spiral initially becomes more elliptical and eventually becomes less elliptical until the particle has finally approached the critical angles.

REFERENCES

[1] B. Kazemi and J. Darabi, Phys. Fluids **30**, 102003 (2018).
[2] T. Jiang, Y. Ren, W. Liu, D. Tang, Y. Tao, R. Xue, and H. Jiang, Phys. Fluids **30**, 112003 (2018).
[3] M. Doi and M. Makino, Phys. Fluids **28**, 093302 (2016).
[4] J. Svoboda and T. Fujita, Miner. Eng. **16**, 785 (2003).
[5] R. D. Ambashta and M. Sillanpää, J. Hazard. Mater. **180**, 38 (2010).
[6] I. Šafařík and M. Šafaříková, J. Chromatogr. B: Biomed. Sci. Appl. **722**, 33 (1999).
[7] M. O. Aviles, H. Chen, A. D. Ebner, A. J. Rosengart, M. D. Kaminski, and J. A. Ritter, J. Magn. Magn. Mater. **311**, 306 (2007).
[8] A. S. Lübbe, C. Alexiou, and C. Bergemann, J. Surg. Res. **95**, 200 (2001).
[9] A. D. Grief and G. Richardson, J. Magn. Magn. Mater. **293**, 455 (2005).
[10] M. Alam, M. Golozar, and J. Darabi, Phys. Fluids **30**, 042001 (2018).
[11] R. Zhou, C. A. Sobecki, J. Zhang, Y. Zhang, and C. Wang, Phys. Rev. Appl. **8**, 024019 (2017).
[12] C. A. Sobecki, J. Zhang, Y. Zhang, and C. Wang, Phys. Rev. Fluids **3**, 084201 (2018).
[13] D. Matsunaga, A. Zöttl, F. Meng, R. Golestanian, and J. M. Yeomans, IMA J. Appl. Math. **83**, 767 (2018).
[14] J. Zhang, C. A. Sobecki, Y. Zhang, and C. Wang, Microfluid. Nanofluid. **22**, 83 (2018).
[15] E. Gavze and M. Shapiro, Int. J. Multiphase Flow **23**, 155–182 (1997).
[16] L. G. Leal, Annu. Rev. Fluid Mech. **12**, 435–476 (1980).
[17] J. A. Stratton, *Electromagnetic Theory* (John Wiley & Sons, 2007).
[18] A. H. Santos, D. Liu, and H. Zhang, *Microfluidics for Pharmaceutical Applications: From Nano/Micro Systems Fabrication to Controlled Drug Delivery* (William Andrew, 2018).
[19] A. Okagawa, R. G. Cox, and S. G. Mason, J. Colloid Interface Sci. **47**, 536 (1974).
[20] Y. Almog and I. Frankel, J. Fluid Mech. **289**, 243 (1995).
[21] D. Matsunaga, F. Meng, A. Zöttl, R. Golestanian, and J. M. Yeomans, Phys. Rev. Lett. **119**, 198002 (2017).
[22] I. Torres-Díaz and C. Rinaldi, J. Phys. D: Appl. Phys. **47**, 235003 (2014).
[23] J. Jezek and S. A. Gilder, J. Geophys. Res.: Solid Earth **111**, B12S23, https://doi.org/10.1029/2006jb004541 (2006).
[24] S. T. Demetriades, J. Chem. Phys. **29**, 1054 (1958).
[25] G. B. Jeffery, Proc. R. Soc. A **102**, 161 (1922).
[26] A. D. Shine and R. C. Armstrong, Rheol. Acta **26**, 152 (1987).
[27] L. J. Reed and E. Tryggvason, Tectonophysics **24**, 85 (1974).
[28] L. Arbaret, N. S. Mancktelow, and J. P. Burg, J. Struct. Geol. **23**, 113 (2001).
[29] N. C. Gay, Tectonophysics **5**, 81 (1968).

Published under license by AIP Publishing